3.5

GASIFICATION ASH AND SLAG CHARACTERIZATION

Quarterly Technical Progress Report
for the Period January - March 1988,
and Final Technical Report for the
Period April 1987 - March 1988

DOE/MC/10637--2827-Task-3.5

DE90 011398

Principal Investigator:

David P. Kalmanovitch

Associated Personnel:

Julie R. Weinmann
Sumitra R. Ness
Steven A. Benson

Work Performed Under Cooperative Agreement
No. DE-FC21-86MC10637

for

U.S. Department of Energy
Office of Fossil Energy
Morgantown Energy Technology Center
Morgantown, West Virginia

by

University of North Dakota
Energy and Mineral Research Center
Grand Forks, North Dakota

DISCLAIMER

TABLE OF CONTENTS

LIST OF FIGURES

LIST OF TABLES

GASIFICATION ASH AND SLAG CHARACTERIZATION

EXECUTIVE SUMMARY

The formation, physical properties, and behavior of ash in coal gasification systems can have a major impact on the design and subsequent operation of the system. Indeed, the behavior of the ash has to be considered in order to decide whether a given coal is suitable for utilization in a given gasification system. The overall objective of the program is to obtain laboratory- and bench-scale data on the formation, flow, and sticking behavior of coal ash and slag under gasification conditions. The eventual outcome will be a unified picture of the behavior of inorganic species within the gasifier. This will include a set of models with which the behavior of an ash can be successfully predicted. The unified picture will be invaluable to the designers and gasifier operators in assessing a coal for utilization in gasification systems.

This report covers the period April 1987 to March 1988, and includes the quarterly progress report for the period January to March 1988. The accomplishments include the study of the mineral transformation of seventeen coal ashes and model mineral mixtures and the determination of the viscosity of two model mineral mixtures and Illinois #6 ash under reducing conditions. The modeling of the behavior of viscosity as a function of temperature involved the compilation of viscosity temperature data of a wide range of molten ashes and glasses. Up to 2000 data sets were compiled. Some data were found to fit very poorly with the viscosity model adopted. These data were identified and removed from the data base. Surface tension was determined on four samples using the sessile drop method. These samples include three coal ashes and a model mineral (sodium montmorillonite). Work was also carried out on the shakedown and performance testing of the pressure pyrolysis unit. This unit was used to prepare char from a suite of coals at ambient pressure and 850^{o}C (10% H_2, 90% N_2).

The coals studied during this reporting period were: Velva lignite, Wyodak subbituminous, Indian Head lignite, Martin Lake lignite, Pittsburgh No. 8 bituminous, and Illinois No. 6 bituminous. The Velva, Wyodak, Indian Head, Martin Lake, and Pittsburgh No. 8 coals were chosen for detailed study as these coals are to be tested in a pilot-scale fluidized bed gasifier at UNDEMRC under a separate program sponsored by METC. Comparison of data obtained from the laboratory-scale study of these coals to the results obtained from the characterization of the bed material and associated agglomerates from the pilot-scale data is planned. This will show the significance of laboratory-scale data and derived models to industrial and pilot-scale gasification projects.

1.0 OBJECTIVES

The overall objective of this project is to develop a unified picture of the ash formation and behavior in coal gasification systems. In particular, the project aims to provide data on the behavior of ash and how it affects gasifier operation. The project is divided into four tasks.

The first task involves the characterization and identification of mechanisms responsible for the complex mineral transformations that coal minerals exhibit under gasification systems. This involves the generation of ash and slag samples in bench-scale and pilot-scale units simulating gasification environments using both high- and low-rank coals. In addition, model mixtures of minerals common to coal, acetic acid salts of various alkali and alkaline earth elements, and iron oxalate will be studied under simulated gasification systems in the laboratory. The use of model mineral mixtures will give baseline data on mineral transformations under well-controlled conditions. The inclusion of mineral mixtures with additions of acetic acid salts will permit study of the effects of organically bound metals on mineral transformations. It must be remembered that, for western coals, some elements are present within the organic matrix of the coal. The effect of the behavior of these elements, usually Na, Mg, and Ca, on the mineral transformation must be understood in order to be able to properly predict the formation and behavior of ash in a gasifier and how the ash may affect gasifier performance. Model mineral mixtures with additions of potassium acetate will also be studied. This is necessary as potassium has been identified as an element which has catalytic activity during coal gasification. Therefore, the effect of potassium on mineral transformation and its characteristics within the product may have a bearing on the behavior of the element as a catalyst.

The second task involves the study of vaporization of inorganic constituents during gasification processes. This includes the use of a computer simulation of solid-gas-liquid phase equilibria in high-pressure, high-temperature systems. Relevant experimental data will be provided by the preparation of coal chars in a pressure pyrolysis unit under carefully controlled conditions. In addition, the chemical composition data from samples studied in the first task will provide data on the loss of inorganics during preparation of ash and slag samples.

The third task evaluates slag viscosity behavior under reducing conditions. The task involves the study of compositional and rheological properties of slag produced from both reduced and oxidized coal ashes and the development of a predictive viscosity model. Of particular importance is the modeling effort to predict the Newtonian flow temperature regime and the effect of crystallization within the slag on bulk flow properties. Viscosities will be determined for coal ashes produced under reducing and oxidizing conditions, model mineral mixtures, and coal ashes with additives. All viscosities are determined under reducing atmosphere.

The fourth task involves the determination and subsequent modeling of surface tension of coal ashes. The surface tension of various coal ashes and model mixtures will be determined under gasification environments on vitreous carbon substrates.

The objectives for this reporting period were to:

1. Complete coal and mineral mixture transformation studies.

2. Prepare and analyze chars from a suite of coals using pressure pyrolysis unit.

3. Obtain, install, and evaluate computer codes (SOLGASMIX and PACKAGE) for determining high-temperature, high-pressure phase equilibrium.

4. Determine viscosity of coal ashes and model mineral mixtures.

5. Develop viscosity model with measured viscosities.

6. Continue modeling effort of viscosity of silicate melts.

7. Determine surface tension of coal ashes and model mineral mixtures.

8. Compile surface tension data base for wide range of alumino slags.

2.0 BACKGROUND STATEMENT

The behavior of ash in coal gasification systems is at present not well understood. Unlike coal combustion systems, where well-defined analytical tests can be used to evaluate a given coal ash in terms of the effect of the ash on combustor performance, there are no similar techniques specific to coal gasification. Indeed, while it is acknowledged that there are significant differences between the environment in a gasifier and that in a coal combustor, gasifier operators and designers use prediction techniques of ash behavior developed for combustors. While the major ash-related problem in a combustor is the formation of fireside deposits on heat transfer surfaces, the operation of a gasifier is directly related to the formation and behavior of the ash. This is because the gasifier, be it dry or slagging type, requires the removal of ash material in order to maintain production. Therefore, it is necessary to establish which characteristics of coal ash formed in a gasifier affect the actual operation and gas production.

In order to obtain this information, it is important to be able to understand by means of laboratory-, bench-, and pilot-scale experiments the complex processes that coal ash species undergo within a gasifier and how they relate to the physical properties of the ash under specific gasification conditions.

2.1 Task A. Mineral Transformations

Coal is a relatively dirty fuel compared to oil. It contains a complex mixture of inorganic mineral matter as well as, particularly for western coals, organically associated inorganic elements. The mode of occurrence, specific chemical and crystalline structure, and the spatial distribution of these minerals can all have an effect on the ash species produced as the residue of coal gasification. Usually the chemical composition of the ash produced from a sample of the feed coal under oxidizing conditions is the only analytical data which is used to characterize this ash. However, the bulk chemical composition does not provide sufficient insight on the behavior of the coal ash within the gasifier.

Therefore, it is necessary to determine the characteristics of ash formed under gasification conditions and to model the behavior. These characteristics include the distribution of phases as a function of temperature and gas composition. The coal ash experiments need to be performed under controlled conditions.

2.2 Task B. Volatilization Studies

A major aspect of the operation of a coal gasification system is predicting the chemical composition of the ash formed in the gasifier. Normal laboratory ashing techniques do not necessarily produce ash which is comparable to that formed in a gasifier. A particular concern is the loss of species from the ash matrix due to volatilization. This will have a direct effect on the bulk chemical composition of the ash and may have an effect on the catalytic activity of certain elements during gasification. Of course, the loss of species due to volatilization will depend on the distribution and origin of the species as well as gasification conditions. Therefore, it is important to understand chemical as well as mineralogical transformations that occur within coal during gasification. In order to establish the degree of volatilization, detailed laboratory experiments have to be performed. High-pressure pyrolysis of coal is a technique which is capable of obtaining data on the volatilization of coal ash species under a wide range of temperature, pressure, and gaseous conditions. The complex nature of volatilization requires detailed modeling studies. This modeling is best accomplished using thermochemical techniques. SOLGASMIX using a data base developed for volatilization studies of coal ash in magnetohydrodynamic systems appears to be best suited for this purpose. Detailed evaluation of the program and how it relates to gasification systems is a crucial aspect to the development of a model of inorganic volatilization during gasification.

2.3 Task C. Viscositiy Studies

Ash in gasification systems is removed either as a granular or powdered material or as molten slag. For a given gasifier operation, it is necessary for the ash to be in the correct form in order to remove the material during normal operation. That is, for dry-bottom gasifiers the ash has to remain granular or in powder form and for wet-bottom or slagging gasifiers the ash has to form a molten slag of sufficiently low viscosity that the material will flow at the slag exit temperature. The extent to which ash melts and agglomerates to form granular or molten slag material is dependent on the chemical, and mineralogical nature of the ash and the temperature, time, and atmospheric conditions it experiences. However, insight into the behavior can be derived from coal ash deposition studies in combustion systems. These studies have identified a mechanism of sintering by viscous flow as that responsible for the formation and growth of ash deposits. This relation has been described by Raask (1) and is given by:

$$\frac{ds}{dt} = \frac{3 \gamma k}{2r \eta}$$

where ds/dt represents the rate of increase in strength, k is a constant, r is the radius of the particles, and γ and η are the surface tension and viscosity of the liquid phase respectively. Note that the relation is given for a system at constant temperature.

For a given ash system, the viscosity of the liquid phase tends to be the major parameter for the sintering process. The higher the viscosity, the lower the rate of sintering, and vice versa. The effect of surface tension on

sintering will be discussed below. Therefore, the degree of sintering is dependent on the viscosity and relative amount of the liquid phase. For slagging systems, the bulk of the ash melt formed flows through a slag tap. In this case, the viscosity of the bulk material is a controlling factor. The bulk viscosity will be dependent on the chemical composition and the temperature. In some cases, crystallization occurs within the melt. This has two effects: first, it reduces the amount of liquid phase present; and second, it alters the chemical composition of the melt. Both of these effects can alter the bulk flow properties. In dry-bottom systems, sintering occurs to a lesser extent than in the slagging gasifier. Here the ash species may form a liquid phase which has a very different composition than the bulk composition. In this case the degree of sintering, at a given temperature, will be dependent on the amount of liquid phase formed, the chemical composition, and the viscosity (as well as the surface tension). The greater the amount of liquid phase formed and the lower the viscosity of the liquid, the greater the degree of sintering. In the dry-bottom system, it is important to limit the degree of sintering to prevent excessive clinkering (formation of large agglomerates). This can only be achieved by the reduction of the amount of liquid phase and/or the viscosity of the liquid phase involved in the sintering. Crystallization can also occur in the ash samples within the dry-bottom gasifier. This will tend to reduce the amount of liquid phase and alter the chemical composition (and hence viscosity) of the component liquid phase.

Therefore, the determination, and indeed the modeling, of the viscous flow behavior of coal ashes as well as possible component liquid phases is important to the understanding of the behavior of a given ash under gasification conditions. Various models of coal ash viscosity have been developed. However, these tend to be rank-dependent and empirically based. Furthermore, they give relatively limited insight into the viscous flow behavior of component liquid phases formed under less extreme conditions. Another factor is that the models have been developed for coal combustion systems and the models use coal ash as the basis of predicting behavior. Schobert et al. (2) have compared the measured viscosity under reducing conditions of a range of molten low-rank coal ashes with the various models available. They found that the empirical models of Watt & Fereday (3) and Reid and Cohen (4) did not fit the measured data well. The explanation was that the methods were based on bituminous coal ashes and include only the concentrations of SiO_2, Al_2O_3, Fe_2O_3, CaO, and MgO. The study showed that the computational method of Urbain gave the best results. The Urbain method has a number of features which make it very attractive to the study of ash behavior. First, it includes all components; second, it is based on the viscosity behavior of silicate melts (it was developed for metallurgical slags); third, it uses mole fraction of components; and fourth, it uses the Frenkel relationship (5) as opposed to the Arrhenius relation. The use of all components ensures that the method is not constrained by a compositional range. The method is also enhanced because the basis of the technique is the flow properties of silicate melts and not those of coal ashes. Certainly, the component liquid phases within an ash are silicate based but may be far removed, in a chemical sense, from coal ashes. Silicate viscosity models use a structure which defines a component oxide as network former, network modifier, or amphoteric. In general, the higher the level of network former, the greater the degree of polymerization within the melt and the higher the viscosity (at a given temperature). Network modifiers tend to reduce the degree of polymerization and hence reduce viscosity.

Amphoteric components can act both as network former or modifier, the role depending on the relative level. In the case of coal ashes, the classification of the component oxides are:

Network former: SiO_2, TiO_2
Network modifier: CaO, MgO, Na_2O, K_2O, FeO
Amphoteric: Al_2O_3, Fe_2O_3

The role of SO_3 is not defined in this model.

The use of mole fractions is a direct consequence of the use of this model. That is, the effect or role of a component oxide will depend on the relative amount of molecules available and not on the relative weight percent. The use of the Frenkel (5) model:

$$\text{viscosity}=A\text{Texp}(E/RT)$$

has been found to give better results than the Arrhenius relationship:

$$\text{viscosity}=A\text{exp}(E/RT).$$

Schobert (2) used the Urbain model as the basis of a modified Urbain viscosity calculation. However, as the focus was on the bulk flow properties of low-rank coal ash slags from a slagging gasifier, the method developed was rank dependent and gave very little insight into the flow properties of component liquid phase.

For this study, the original Urbain method was used as the basis of a modeling effort. A unique feature of this project was the use of model mixtures as well as the preparation of a computer data base of the viscosity of silicate melts. These melts include glasses from simple oxide systems. The basis of this was straightforward. In order to be able to predict the flow properties of a complex aluminosilicate melt (coal ash), it is necessary to be able to model the viscosity of simpler systems. That is, the model should be applicable to both simple oxide melts and complex oxide melts. This has the added benefit of being able to determine the viscosity of residual liquid phases and component liquid phases as well as bulk properties. That is, if the crystallization behavior or partitioning of various components is known, then the effect of these processes on the sintering or bulk flow properties can be predicted.

There are a number of experimental aspects to this project, including the determination of viscosity/temperature relationships for a number of coal ashes under reducing conditions, the determination of viscosity/temperature curves for model mixtures, and the development of a data base on viscosity of coal ashes (all ranks), model mixtures, and simple oxide glasses. All of this data is necessary in order to be able to model the viscous flow behavior of coal ashes in gasification systems.

2.4 Task D. Surface Tension

The surface tension is the measure of the relative wetting characteristics of a material on a substrate. In gasification systems, surface tension of the slag or component liquid phase can affect the rate of sintering, formation of

slag, or the attack of refractory components. That is, for slagging units a low-ash particle-to-ash particle surface tension is required to enhance capture and assimilation within the slag. However, a high surface tension is required between the slag and the refractory to reduce attack or corrosion of the refractory. For dry-bottom systems, a high particle-to-particle surface tension reduces the initial adhesion of contacting particles and hence reduces agglomeration.

Therefore, the surface tension of ash melts and component liquid phases can have an important effect on the operation of a gasifier. It is necessary to be able to model the surface tension of the slags. In order to do this, the surface tension of a number of coal ash slags and model mixtures will be measured under reducing conditions. As the substrate in surface tension experiments can have an effect on the surface tension, it was decided to measure the surface tension on an inert substrate. In this study, vitreous carbon was used. The method used to determine the surface tension was the sessile drop method, which involves the determination of the shape of a slag bead on a substrate at elevated temperatures.

3.0 PROJECT DESCRIPTION

3.1 Task A. Mineral Transformations

Table 1 lists the coal ashes and model mixtures studied in this project. Each of the coal samples was treated at 1000°C under both oxidizing (air) and reducing (92%N_2, 8%H_2) conditions for three hours and are referred to as high-temperature ashes (HTA). All model mineral mixtures were ground to -60 mesh, thoroughly mixed in a ball mill, and treated at 1000°C for 3 hours. All the samples were submitted for bulk chemical analysis (x-ray fluorescence) and crystalline phase assemblage (powder x-ray diffraction). The model mixtures were also analyzed by x-ray fluorescence before treatment. Detailed information of the chemical transformation of the samples and mineralogical phases formed was obtained using a technique called Scanning Electron Microscopy Point Count (SEMPC). This novel technique was developed at UNDEMRC specifically to determine, quantitatively, the phases present and the respective compositions in coal ash systems. The data gives unique insight into the composition of amorphous phases present.

The analytical data from slags produced in the viscosity studies of Task C were also used in this task.

3.2 Task B. Volatilization Studies

Pressure pyrolysis of coals was used to obtain data on the degree of volatilization of various components under gasification conditions. A schematic of the pressure pyrolysis unit is given in Figure 1. The unit is used to prepare chars from coals at a variety of temperatures and pressures. The coals to be studied and the various conditions used to prepare chars are given in Table 2. Samples of -60 mesh coal are placed in crucibles and placed in the reactor. The temperature and pressure are adjusted to run conditions and are held constant for 3 hours. Samples are submitted for detailed computer-controlled scanning electron microscope analysis using SEMPC to determine the amount and composition of the mineral phases. The char is then ashed in the low-temperature ash unit and submitted for X-ray fluorescence

TABLE 1

COAL ASHES AND MODEL MINERAL MIXTURES STUDIED IN TASK A

Coal/Mineral Mixture	Rank/Proportion (mol/mol)
Illinois No. 6	Bituminous
Indian Head	Lignite
Martin Lake	Lignite
Pittsburgh No. 8	Bituminous
Wyodak	Subbituminous
Velva	Lignite
Kaolinite	Pure
Kaolinite + Iron (II) Oxalate	1:1
Kaolinite + Calcium Acetate	1:1
Kaolinite + Calcium Acetate	1:2
Kaolinite + Magnesium Acetate	1:1
Kaolinite + Potassium Acetate	1:1
Kaolinite + Sodium Acetate	1:1
Sodium Montmorillonite	Pure
Sodium Montmorillonite + Iron (II) Oxalate	1:1
Sodium Montmorillonite + Aluminum Acetate	1:1
Sodium Montmorillonite + Calcium Acetate	1:1
Sodium Montmorillonite + Potassium Acetate	1:1
Sodium Montmorillonite + Sodium Acetate	1:1
Kaolinite + Sodium Acetate + Quartz	1:1:2
Kaolinite + Potassium Acetate + Quartz	1:1:2
Kaolinite + Iron (II) Oxalate + Quartz	1:1:1
Kaolinite + Magnesium Acetate + Quartz	1:1:1
Illite + Calcium Acetate	1:1
Illite + Iron (II) Oxalate	1:1
Illite + Potassium Acetate	1:1
Illite + Magnesium Acetate	1:1
Illite + Sodium Acetate	1:1
Calcium Montmorillonite	Pure
Calcium Montmorillonite + Calcium Acetate	1:1
Calcium Montmorillonite + Magnesium Acetate	1:1
Calcium Montmorillonite + Sodium Acetate	1:1
Calcium Montmorillonite + Iron (II) Oxalate	1:1
Calcium Montmorillonite + Potassium Acetate	1:1

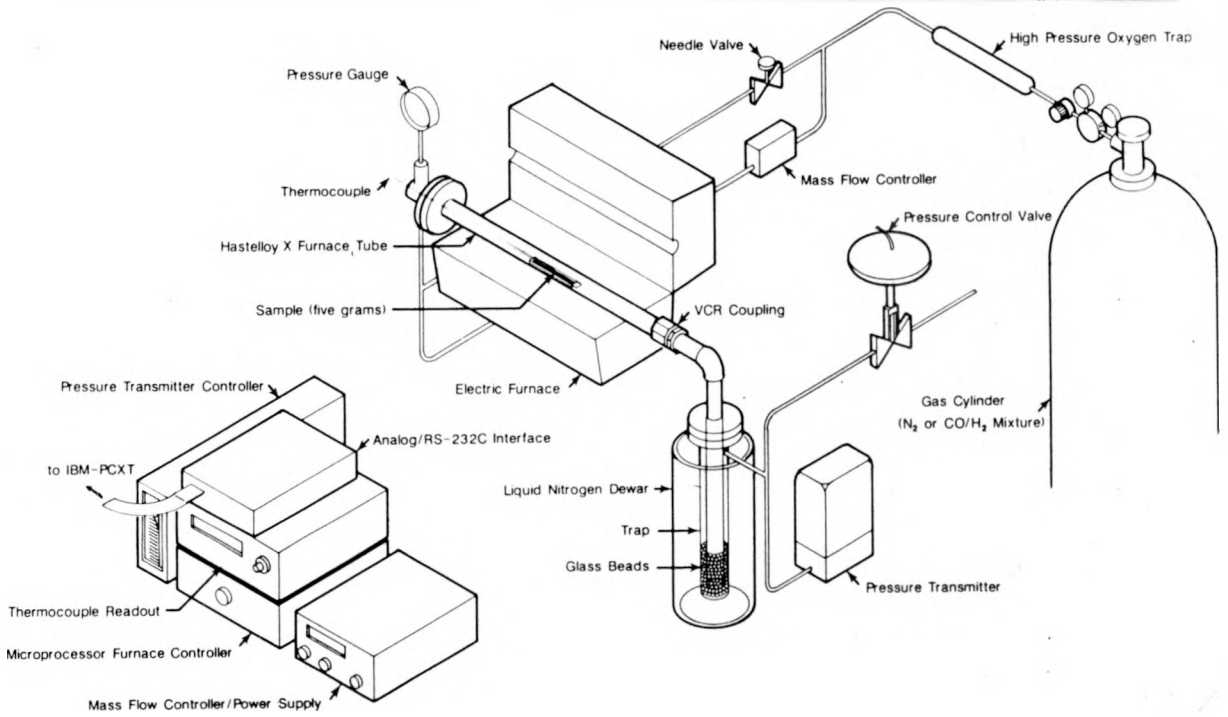

Figure 1. Schematic Diagram of the Pressure Pyrolysis Unit

TABLE 2

TEST MATRIX: PRESSURE PYROLYSIS

Coal	Pressure (psi)	Temperature (°C)
Illinois No.6	14.7, 200, 400	850
Indian Head	14.7, 200, 400	850
Martin Lake	14.7, 200, 400	850
Pittsburgh No. 8	14.7, 200, 400	850
Wyodak	14.7, 200, 400	850
Velva	14.7, 200, 400	850

(XRF) and X-ray diffraction (XRD) analysis to determine chemical composition and crystalline phase assemblage, respectively.

The data, i.e., the change in chemical composition and mineral transformation, will be modeled using thermochemical techniques. These techniques, such as SOLGASMIX (6) and PACKAGE (7), were developed to determine or predict phases in hostile environments. For example, SOLGASMIX has been applied to the analysis of the behavior of potassium within the plasma of MHD systems (temperature of over 2000 K). PACKAGE was derived from the NASA CEC code. The precursor was developed for the study of rocket flames and emissions. With respect of coal utilization systems, SOLGASMIX and its derivatives appear

to have been used more often by researchers than PACKAGE. Indeed, a version of SOLGASMIX is part of the PCGC-2 modeling effort at Brigham Young University, as well as researchers at Argonne, MIT, PSI, and NBS. PACKAGE is used by researchers at Morgantown Energy Technology Center (METC) and at Aerodyne Research Corporation.

Both programs were made available to UNDEMRC. A recent mainframe version of SOLGASMIX was supplied by Dr. Bonnel of NBS. PACKAGE was supplied by Dr. Nagarajan of METC. Due to previous experience with SOLGASMIX, it was decided to initially use SOLGASMIX for thermochemical predictions and modeling of phase equilibria in gasification systems.

3.3 Task C. Viscosity Studies

The viscosity of coal ashes and model mineral mixtures was determined using a rotating bob viscometer. A schematic of the viscometer apparatus is given in Figure 2. The gas flow through the viscometer was controlled to produce an atmosphere of 8% hydrogen and 92% nitrogen. Viscosities in the range 1 to 3000 poise (0.1 to 300 Pa s) could be measured. Both oxidized and reduced HTA from Task A were used as the starting material for the viscosity studies of coal ashes. Reduced HTA was used for the mineral mixtures. In some cases, slag was prepared from the HTA (oxidized and reduced) of the coals in a separate furnace. This was done to prevent excessive frothing of the sample in the viscometer. After determination of the viscosity/temperature relationship of the sample (cooling cycle), the furnace was cooled and the sample removed. The samples were then subjected to x-ray fluorescence, x-ray diffraction, and scanning electron microscopy analysis using the SEMPC. For the viscometer samples, the analysis was focused on verifying that the sample was homogeneous. Work was also focused on the composition of the crystalline phases present and the relative amount of the phases. An advantage of the SEMPC technique is that it is able to determine the chemical composition, using microprobe data, of both amorphous and crystalline phases present in a sample. Details of the technique can be found elsewhere. The results of these analyses are required to:

1. model the crystallization behavior of slags, and

2. relate the crystallization behavior to bulk flow properties.

The viscosity data from this task is part of an extensive data base of viscosity/temperature data. This data base will be used to develop a model to predict flow properties both in the Newtonian and non-Newtonian regimes. Unlike other attempts to model ash viscosity (for example Watt and Fereday (3), and Sage and McIlroy (8), the data base includes, in addition to results from this task, viscosity data from all ranks of coal, simple oxide glasses and geological samples. As discussed in a previous report (9), the model to be used will be that of Urbain (10). The model has a number of advantages over other models, including the incorporation of all components and a theoretical model of the structure of silicate melts. Since the model will not be restricted to a specific range of ash compositions, as is the case with most empirical models of coal ash viscosity, it can be used to determine bulk flow as well as the viscosity of component liquid phases. The study involves the compilation of viscosity, chemical composition, and temperature data and associated analyses including statistical correlations.

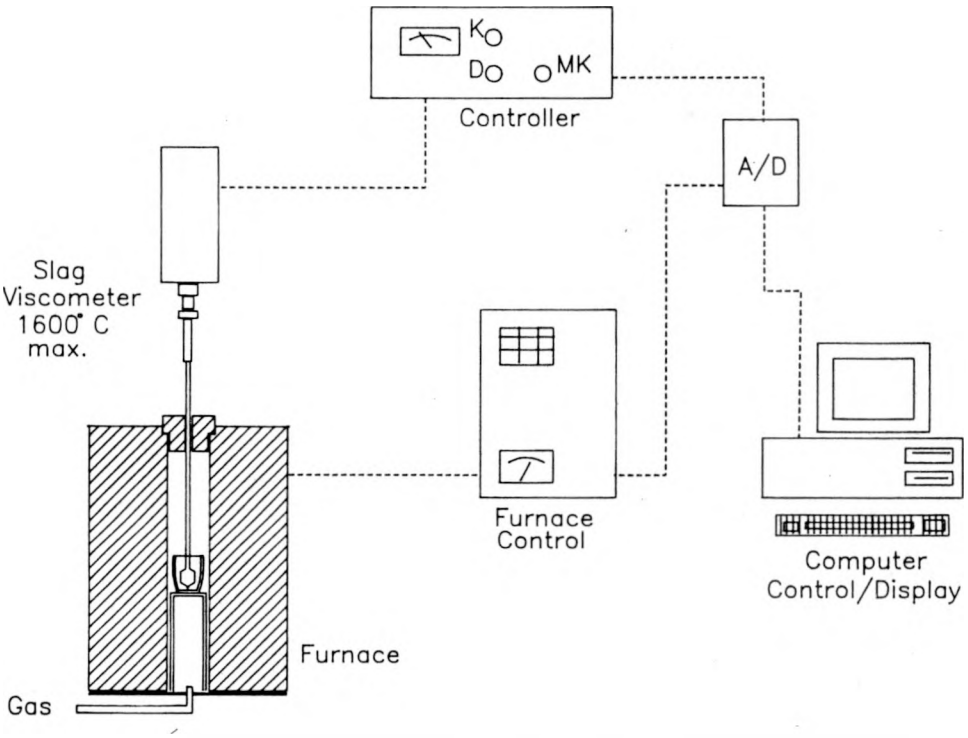

Figure 2. Schematic of High-Temperature Rotating Bob Viscometer

A key aspect is the prediction of the crystallization behavior of coal ash melts. This is important, as the crystallization directly affects the composition of the component liquid phases. Indeed, the relative amount of crystalline phases can have a direct influence on the sintering or even bulk flow properties of slags. While most models of viscosity cover the Newtonian range, there is a need to understand the bulk flow properties of slags after the onset of crystallization. This requires the modeling of the crystallization behavior of slags. Studies by Kalmanovitch and Williamson (11) have shown the applicability of equilibrium phase diagrams to crystallization in coal ash systems. These diagrams will be used in conjunction with a thermochemical equilibrium program (SOLGASMIX) and crystallization data from the viscosity tests in the development of a model of crystallization behavior of slags. This model, combined with the model to predict Newtonian flow behavior of slags, will be used to develop an overall model of bulk flow properties of slags. The final model will also have direct applicability to the understanding of ash sintering behavior in dry-bottom gasifiers.

In order to model the crystallization behavior, detailed information on the phases present must be obtained. This requires the use of SEMPC to determine both the relative amount of phases and the composition of the phases present in the slag samples.

3.4 Task D. Surface Tension

The surface tension of a liquid or melt is the measure of the degree of "wetting" of an adjacent (usually solid) surface the liquid exhibits. A high surface tension results in a non-wetting liquid material. In this case, the liquid will form a spherical bead on the surface of the substrate. A low

surface tension results in wetting of the substrate with the liquid covering a large area of the substrate. The surface tension is important to the study of ash behavior in gasification systems. It affects the interaction of molten slag with gasifier surfaces, as well as the fundamental sintering process. In the latter, the surface tension of the liquid phase on the surface of an ash particle affects the initial adhesion of particles. After adhesion, the surface tension forces pull the liquid phase to the neck region, enhancing the sintering process. In the first case, the low surface tension enhances adhesion between contacting particles. However, sintering is enhanced by high surface tension.

The technique used for the determination of surface tension chosen for this study was the sessile drop technique. The technique involves the melting of a slag (completely molten sample) previously prepared by grinding and pressing into a pellet of known dimensions. The pellet is mounted on vitreous carbon (inert substrate) and heated in a horizontal furnace under controlled atmospheric conditions. The change in shape as the pellet melts and tries to form a symmetrical bead on the carbon is recorded using a camera. The photograph which shows the symmetrical bead is then analyzed to determine the dimensions of the bead. From these dimensions, the surface tension can be calculated. The temperature at which the sample formed the bead is also recorded. A schematic of the apparatus used and the dimensions of the bead measure are shown in Figures 3 and 4. In this study, the surface tension is determined under reducing atmosphere. The surface tension will be measured for all the coal ashes and model mineral mixtures in Task A (Mineral Transformations). Analysis of the samples will include x-ray diffraction, scanning electron microscopy with electron microprobe. Specific interest will be focused on the crystallization effects and the composition of the surface liquid phase.

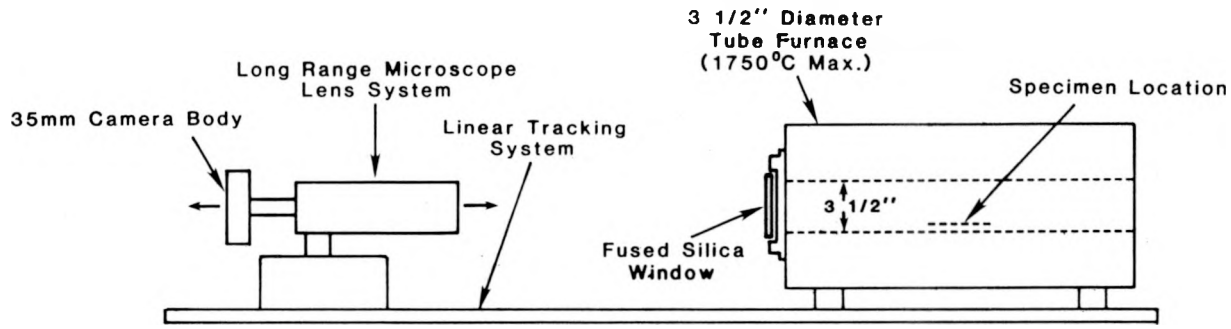

Figure 3. UNDEMRC Surface Tension Apparatus

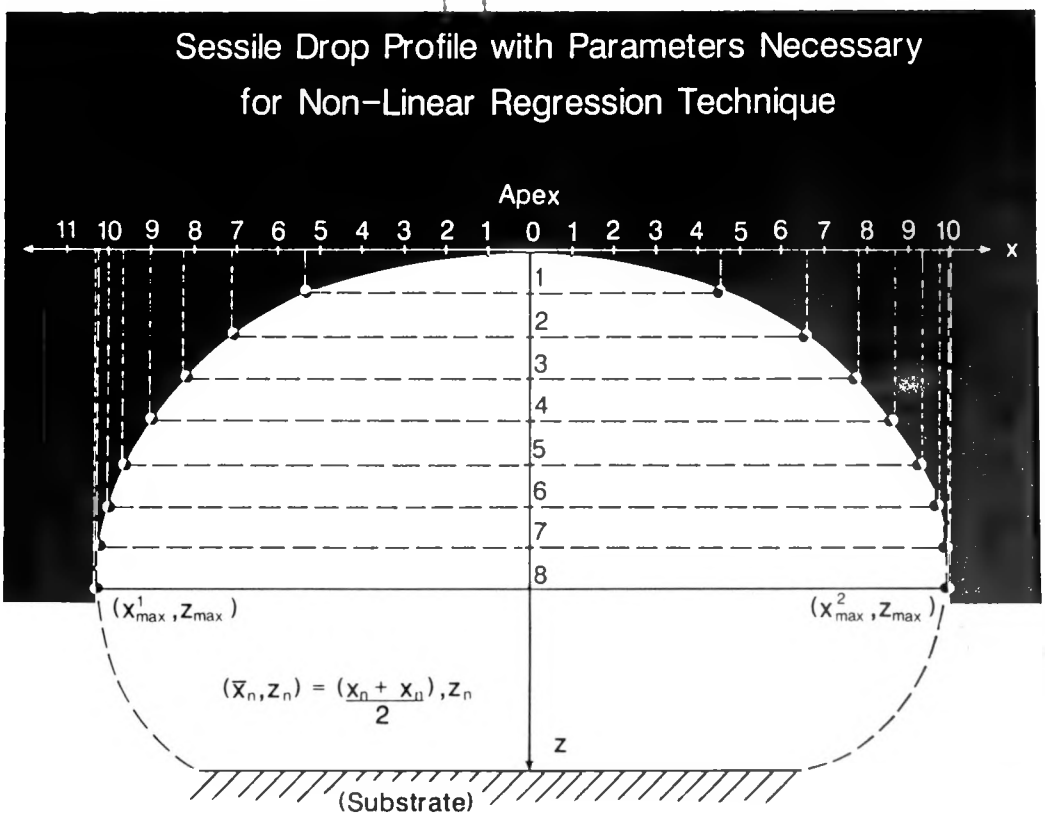

Figure 4. Schematic of Surface Tension Bead

4.0 RESULTS/ACCOMPLISHMENTS

4.1 Task A. Mineral Transformations

Tables 3 and 4 list the chemical composition of the coal ash and slag samples, respectively, studied in this Task. Also included are the results of the x-ray diffraction analysis of the samples. In all relevant cases, the chemical composition for each sample has also been converted to composition on an SO_3-free basis. This allows comparison of the relative levels of the metal oxide components. In some cases, Tables 3 and 4 are incomplete, as the study is still ongoing. However, the study of the coals has been completed and all the data have been compiled. While detailed correlations of the data will be undertaken in the near future, certain interesting observations should be noted. In general, the oxidized high-temperature ashes have a very different crystalline phase assemblage than the high-temperature ashes produced under a reducing atmosphere (8% hydrogen, 92% nitrogen). The bituminous coals (Illinois No.6 and Pittsburgh No.8) tend not to have complex aluminosilicate phases in the HTAs under either condition. The crystalline phases observed for these ashes tend to be simple oxides derived from the thermal decomposition of mineral species. In contrast, the low-rank coals tend to have simple oxides, sulfate species, and complex silicate (such as melilite, pyroxene, and plagioclase) crystalline species present in the HTA samples. The complex silicate species are usually formed by a crystallization process from a molten phase. This indicates that the low-rank coals tend to exhibit more melting and interaction than the bituminous coals during the ashing process. Another important observation is the presence of sulfide species formed in the slags

TABLE 3

TRANSFORMATION DATA: COAL ASHES

COAL ASH	SiO_2	Al_2O_3	Fe_2O_3	TiO_2	P_2O_5	CaO	MgO	Na_2O	K_2O	SO_3
ILLINOIS No.6										
OXATM	29.3	18.8	3.9	1.9	1.7	23.9	7.4	1.0	0.3	11.8
*	33.1	21.3	4.4	2.2	1.9	27.1	8.4	1.1	0.3	--
MINERALOGY	Quartz(m) Hematite(M) Magnetite(M) Anorthite(t)									
REDATM	36.3	16.5	3.8	1.8	1.2	23.8	5.5	0.	0.3	9.9
*	40.2	18.3	4.2	2.0	1.3	26.4	6.1	1.0	0.3	--
MINERALOGY	Quartz(M) Hematite(M) Anorthite(t)									
INDIAN HEAD										
OXATM	28.1	12.9	9.2	0.9	0.4	26.5	6.8	.4	0.7	12.1
*	31.9	14.7	10.5	1.0	0.5	30.2	7.7	2.7	0.8	--
MINERALOGY	Anhydrite(M) Melilite(M) Magnetite(M) Lime(t) Anorthite(t)									
REDATM	36.0	15.3	10.3	0.9	0.1	22.8	6.5	3.2	1.2	3.7
*	37.3	15.9	10.7	0.9	0.1	23.7	6.8	3.3	1.2	--
MINERALOGY	Melilite(M) Magnesia(M) Pyroxene(M) Anhydrite(M) Quartz(M) Nepheline(M)									
MARTIN LAKE										
OXATM	37.6	14.9	10.4	1.0	0.0	23.3	6.6	2.5	0.8	2.9
*	38.7	15.3	10.7	1.0	0.0	24.0	6.8	2.6	0.8	--
MINERALOGY	Melilite(M) Pyroxene(M) Magnetite(M) Quartz(M) Anorthite(t) Anhydrite(t) Na_2CaSiO_4(t)									
REDATM	22.9	14.0	6.9	1.3	0.8	24.9	7.3	0.9	0.1	20.9
*	29.0	17.7	6.7	1.6	1.0	31.5	9.2	1.1	0.1	--
MINERALOGY	Anhydrite(M) Quartz(M) Hematite(t) Spinel(t)									
PITTSBURGH No.8										
OXATM	50.8	20.2	17.5	1.2	0.3	5.2	1.3	0.0	2.5	1.1
*	51.3	20.4	17.7	1.2	0.3	5.3	1.3	0.0	2.5	--
MINERALOGY	Quartz(M) Hematite(M)									
REDATM	49.3	21.2	16.5	1.1	.4	4.1	1.4	0.0	2.4	3.6
*	51.1	22.0	17.1	1.1	0.4	4.3	1.5	0.0	2.5	--
MINERALOGY	Quartz(M) Hematite(M) Anhydrite(m) Magnetite(m)									
VELVA										
OXATM	22.8	11.4	7.0	0.9	0.5	35.9	8.8	1.7	0.3	10.7
*	25.6	12.8	7.8	1.0	0.6	40.1	9.9	1.9	0.3	--
MINERALOGY	Anhydrite(M) Melilite(M) Magnesia(M) $Ca_4Al_6O_{12}SO_4$(t) $Ca_3Al_2O_6$(t)									
REDATM	32.3	13.3	7.5	1.5	0.0	35.4	8.3	1.1	0.6	0.0
*	32.3	13.3	7.5	1.5	0.0	35.4	8.3	1.1	0.6	0.0
MINERALOGY	Melilite(M) Magnesia(m) Ca_2SiO_4(m)									
WYODAK										
OXATM	29.3	18.8	3.9	1.9	1.7	23.9	7.4	1.0	0.3	11.8
*	3.1	21.3	4.4	2.2	1.9	27.1	8.4	1.1	0.3	
MINERALOGY	Quartz(M) Anhydrite(M) Plagioclase(M) Hauyne(M) Magnesia(t)									
REDATM	36.3	16.5	3.8	1.8	1.2	23.8	5.5	0.9	0.3	9.9
*	40.2	18.3	4.2	2.0	1.3	26.4	6.1	1.0	0.3	--
MINERALOGY	Quartz(M) Anhydrite(M) Hauyne(M)									

KEY: * = SO_3-Free Composition
M = Major Component
m = Minor Component
t = Trace Component

TABLE 4

TRANSFORMATION DATA: COAL SLAGS

COAL SLAGS	SiO_2	Al_2O_3	Fe_2O_3	TiO_2	P_2O_5	CaO	MgO	Na_2O	K_2O	SO_3
ILLINOIS No.6										
OXATM	48.6	23.1	14.3	1.2	0.3	56.4	1.6	0.5	3.1	1.9
*	49.6	23.5	14.6	1.2	0.3	5.5	1.6	0.5	3.2	--
MINERALOGY	Amorphous									
REDATM	55.0	20.4	11.9	1.2	0.0	5.3	1.6	0.8	3.6	0.1
*	55.1	20.4	11.9	1.2	0.0	5.3	1.6	0.8	3.6	--2
MINERALOGY	Anorthite(M) Amorphous(M)									
INDIAN HEAD										
OXATM	36.0	22.1	2.8	1.2	0.1	24.0	5.8	1.9	0.9	5.2
*	38.0	23.3	3.0	1.3	0.1	25.3	6.1	2.0	0.9	--
MINERALOGY	Amorphous(M) FeS(M) CaS(M) Unknown(M)									
RED	33.8	20.9	10.0	0.9	0.3	20.2	4.9	2.8	0.9	5.2
*	35.7	22.1	10.6	1.0	0.3	21.3	5.2	3.0	1.0	--
MINERALOGY	Pyroxene(M) Aluminum Oxide Sulfate(M) Potassium Sulfate(m)									
MARTIN LAKE										
OXID	33.4	19.0	10.4	1.2	0.0	24.9	5.9	1.5	0.4	3.3
*	34.5	19.7	10.8	1.2	25.8	6.1	1.6	0.4	--	
MINERALOGY	CaS(M) FeS(M) Amorphous(M)									
RED	32.9	17.2	7.5	1.7	0.0	25.8	6.2	4.5	0.4	3.8
*	34.2	17.9	7.8	1.8	0.0	26.8	6.4	47	0.4	--
MINERALOGY	Gehlenite/Akermanite(M)									
PITTSBURGH No.8										
OXID	49.5	20.6	17.8	1.3	0.2	5.1	1.1	0.0	2.7	1.7
*	50.3	21.0	18.1	1.3	0.2	5.2	1.1	0.0	2.7	--
MINERALOGY	FeS(M) CaS(M) Amorphous(M)									
REDATM	46.0	21.8	20.3	1.2	0.3	5.4	1.1	0.0	2.4	1.5
*	46.7	22.1	20.6	1.2	0.3	5.5	1.1	0.0	2.4	--
MINERALOGY	Amorphous(M)									
VELVA										
OXATM	24.7	22.8	7.4	0.7	1.1	20.2	5.1	3.2	0.6	14.3
*	28.8	26.6	8.6	0.8	1.3	23.5	5.9	3.7	0.7	--
MINERALOGY	Amorphous(M)									
REDATM	23.6	11.4	7.9	0.9	0.4	35.8	9.8	1.6	0.2	8.4
*	25.7	12.4	8.6	1.0	0.4	39.1	10.7	1.7	0.2	--
MINERALOGY	Melilite(M) Magnesia(m) Ca_2SiO_4(m)									
WYODAK										
OXATM	41.2	20.0	4.65	2.0	0.8	24.1	5.3	1.0	0.5	0.5
*	41.4	20.1	4.6	2.0	0.8	24.2	5.3	1.0	0.5	--
MINERALOGY	Anorthite(M)									
REDATM	40.8	18.1	6.3	1.8	1.1	21.1	5.4	1.3	0.5	3.6
*	42.3	18.8	6.5	1.9	1.1	21.9	5.6	1.3	0.5	--
MINERALOGY	Anorthite(M)									

KEY: * = SO_3-Free Composition
m = Minor Component
M = Major Component
t = Trace Component

from some coals. Both calcium and iron sulfide (CaS and FeS, respectively) were present in the slags (produced under reducing conditions) from oxidized HTAs of some coals (specifically, Martin Lake, Indian Head, and Pittsburgh No.8). This observation was confirmed by SEMPC analysis. The presence of surface species explains, in part, the relatively high sulfur contents of the slags. The samples which exhibit the sulfide phases tend to be those produced from oxidized HTA. This indicates that mineral transformations during ashing are sensitive to temperature, atmosphere, and original mineral matter distribution. Furthermore, the phases within the ash can have a dramatic effect on the phases within slags at higher temperatures. An excellent example of this behavior is that of Martin Lake lignite. Both slag samples had very similar chemical compositions. However, the slag produced from the reduced HTA crystallized melilite, while the slag from the oxidized HTA contained CaS and FeS. Further studies are required to establish the mechanisms of mineral transformations during ashing.

Table 5 lists the chemical composition (SO_3-free) and the mineralogies of the model mineral mixtures. The data shown is quite complex and does not show clear trends. However, by studying each mineral mixture, some behavior can be determined. The mixture kaolinite + iron (II) oxalate did not show significant change in chemical composition during high-temperature ashing and slag formation. However, during high-temperature ashing, there was decomposition of the iron (II) oxalate to iron oxide and melting of the kaolinite. As kaolinite has a high melting point above the ashing temperature, some interaction between the iron and the kaolinite must have occurred. The slag exhibited mullite and iron (II) oxide as crystalline phases. Mullite ($3Al_2O_32SiO_2$) is a product of thermal decomposition of kaolinite. However, as the kaolinite appears to melt in the presence of iron oxide at ashing temperatures (1000°C), the mullite is probably due to recrystallization from the melt. The presence of crystalline iron oxide may be due to heterogeneity of the sample.

The chemical composition for the initial kaolinite and potassium acetate mixture appears to have a higher SiO_2 and lower Al_2O_3 content than the corresponding HTA and slag. However, the other components are present at similar concentrations. Of importance is the K/Si molar ratio. The ratio was the same for all samples (about 0.6). This indicates that the potassium was not lost relative to the major component (SiO_2). X-ray diffraction analysis of the initial mixture showed some quartz present which was presumably an impurity in the clay. The high-temperature ash sample contained K-nepheline ($KAlSiO_4$) as the only crystalline phase in an amorphous matrix. This is due presumably to decomposition of the K-acetate to K_2O, followed by reaction between the K_2O and the clay to form a low-melting liquid phase which then crystallizes K-nepheline. The presence of an unidentified crystalline phase in the slag sample is probably due to equilibrium not being reached.

The initial chemical composition of the kaolinite and calcium acetate model mixture showed a slightly higher SiO_2 and lower Al_2O_3 and CaO content than the high-temperature ash and the slag. The other components were present at similar levels for all the samples. Furthermore, the Ca/Si molar ratio was similar for all three samples, indicating no significant loss of Ca with respect to Si. The HTA contained gehlenite ($2\ CaO.Al_2O_3.SiO_2$) and calcium oxide as major phases with mullite and an unidentified phase observed as minor crystalline phases. The phases are consistent with decomposition of the

TABLE 5

MINERAL TRANSFORMATIONS: MODEL MIXTURES

	SiO_2	Al_2O_3	Fe_2O_3	TiO_2	P_2O_5	CaO	MgO	Na_2O	K_2O	SO_3
KAOLINITE Initial	53.2	41.6	0.5	2.1	0.0	0.4	1.5	0.6	0.1	0.0
KAOLINITE + IRON (II) OXALATE (1:1)										
Initial	49.7	37.9	9.2	1.8	0.0	0.1	1.2	0.0	0.0	0.0
	Kaolinite (M) Iron Oxalate (m)									
HTA-Red	48.7	39.7	8.1	1.8	0.0	0.5	1.2	0.0	0.0	---
	Hermatite (M) Amorphous (M)									
Slag-Red	48.6	38.2	9.2	2.0	0.1	0.4	1.3	0.0	0.1	---
	Mullite (M) Iron Oxide (m)									
KAOLINITE + POTASSIUM ACETATE (1:1)										
Initial	47.8	31.0	0.5	1.9	0.2	0.8	1.1	0.5	21.2	---
	Kaolinite (M) Quartz (M) Potassium Acetate									
HTA-Red	41.7	34.7	0.3	1.9	0.1	0.0	1.2	1.1	18.8	
	K-Nepheline (M) Amorphous (m)									
Slag-Red	42.4	34.3	0.6	1.8	0.1	0.1	1.3	0.9	18.3	
	Unidentified Crystalline Phase									
KAOLINITE + CALCIUM ACETATE (1:1)										
	44.1	30.2	0.5	1.9	0.0	22.4	0.9	0.0	0.0	---
	Kaolinite (M) Calcium Acetate (M)									
HTA-Red	40.3	32.6	0.4	1.6	0.0	24.1	1.0	0.0	0.0	
	Gehlenite (M) CaO (M) Mullite (M) + Unidentified phase (m)									
Slag-Red	41.6	33.0	0.6	1.7	0.0	22.4	0.7	0.0	0.0	
	Anorthite (M) Calcium Carbonate (M) + Hematite (m)									
KAOLINITE + MAGNESIUM ACETATE (1:1)										
Initial	47.5	35.0	0.4	1.8	0.0	0.0	14.6	0.7	0.0	---
	Kaolinite (M) Magnesium Acetate (t)									
HTA-Red	46.8	36.2	0.3	1.7	0.0	0.1	15.8	1.1	0.0	---
	Mullite (M) Spinel (M) Kaolinite (t)									
Slag-Red	45.0	36.0	0.8	1.7	0.0	0.7	13.9	0.9	1.0	---
	Cordierite (M) Spinel (M) Forsterite (m)									
KAOLINITE + SODIUM ACETATE (1:1)										
Initial	43.5	27.8	2.7	1.7	0.0	1.1	0.6	22.6	0.0	---
	Kaolinite (M) Quartz (M) Sodium Acetate (t) + Unidentified									
HTA-Red	46.4	36.2	0.5	1.7	0.2	0.2	1.2	12.9	0.7	---
	Corundum $(M)_2$ Unidentified									
Slag-Red	48.7	37.0	0.5	1.8	0.0	0.2	0.7	11.3	0.2	---
	Corundum (M)									

KEY: * = SO_3-Free Composition
m = Minor Component
M = Major Component
t = Trace Component

TABLE 5 (CONT.)

MINERAL TRANSFORMATIONS: MODEL MIXTURES

	SiO_2	Al_2O_3	Fe_2O_3	TiO_2	P_2O_5	CaO	MgO	Na_2O	K_2O	SO_3
KAOLINITE + CALCIUM ACETATE (1:2)										
Initial	33.1	24.4	1.8	1.6	0.1	38.0	1.0	0.0	0.0	---
	Kaolinite (M) Calcium Acetate (M)									
HTA-Red	33.3	26.0	0.5	1.5	0.0	37.6	1.2	0.0	0.0	---
	Gehlenite (M) CaO (M) Anorthite (M)									
Slag-Red	33.9	26.9	0.5	1.3	0.0	35.7	1.1	0.6	0.0	---
	Anorthite (M) Gehlenite (M)									
KAOLINITE + SODIUM ACETATE + QUARTZ (1:1:2)										
Initial	58.9	28.3	0.2	1.3	0.0	0.0	0.5	10.8	0.0	---
	Sodium Acetate (M) Kaolinite (m) Quartz (t)									
HTA-Red	61.2	29.1	0.4	1.4	0.0	0.1	0.6	7.2	0.0	---
	Nepheline (M) Quartz (M)									
Slag-Red	62.7	28.3	0.9	1.2	0.0	0.0	0.7	6.2	0.0	---
	Quartz (M) Corundum (M)									
KAOLINITE + POTASSIUM ACETATE + QUARTZ (1:1:2)										
Initial	51.6	26.7	0.3	1.7	0.0	1.6	0.6	0.0	17.6	---
	Kaolinite (M) Potassium Acetate (M) Quartz (t)									
HTA-Red	56.2	26.9	0.2	1.3	0.0	1.4	0.8	0.0	15.2	---
	Quartz (M) $Ca_3Al_{10}O_{18}$ (m)									
Slag-Red	59.1	22.4	0.2	1.3	0.0	1.4	0.6	0.0	15.0	---
	$KAlSi_2O_6$ (M) Quartz (M) Corundum (m)									
KAOLINITE + IRON (II) OXALATE + QUARTZ (1:1:1)										
Initial	48.7	27.4	20.9	1.3	0.1	0.5	0.9	0.0	0.1	---
	Kaolinite (M) Iron Oxalate (M) Quartz (m)									
HTA-Red	49.5	30.2	18.0	1.3	0.0	0.2	0.7	0.0	0.1	---
	Hematite (M) Quartz (M)									
Slag-Red (N/A)										
KAOLINITE + MAGNESIUM ACETATE + QUARTZ (1:1:1)										
Initial	52.6	31.1	0.2	1.6	0.0	0.0	13.9	0.8	0.0	---
	Kaolinite (M) Magnesium Acetate (M) Quartz (t)									
HTA-Red	52.6	31.1	0.2	1.6	0.0	0.0	13.9	0.8	0.0	---
	Quartz (M) Spinel (M) Mullite (M)									
Slag-Red	56.2	29.5	0.6	1.5	0.0	0.1	11.7	0.5	0.0	---
	Indialite (M)									

KEY: * = SO_3-Free Composition
M = Major Component
m = Minor Component
t = Trace Component

TABLE 5 (CONT.)

MINERAL TRANSFORMATIONS: MODEL MIXTURES

	SiO_2	Al_2O_3	Fe_2O_3	TiO_2	P_2O_5	CaO	MgO	Na_2O	K_2O	SO_3
ILLITE + CALCIUM ACETATE (1:1)										
Initial	52.1	19.7	7.7	1.1	0.0	11.6	1.8	0.0	6.3	---
	Illite (M) Quartz (M) Calcium Acetate (m)									
HTA-Red	54.4	18.9	7.4	1.1	0.0	10.4	1.7	0.0	6.2	---
	Quartz (M) CaO (m) Anorthite (m) Gehlenite (m)									
Slag-Red (N/A)										
ILLITE + IRON OXALATE (1:1)										
Initial	51.9	19.9	18.3	1.1	0.0	1.1	1.9	0.0	5.7	---
	Illite (M) Quartz (M) Iron Oxalate (M)									
HTA-Red	52.6	19.0	18.4	1.1	0.0	1.2	1.8	0.0	5.9	---
	Quartz (M) Hematite (M)									
Slag-Red	65.9	21.3	3.7	0.1	0.0	1.7	6.8	0.0	0.6	---
	Amorphous (M) Iron Oxide (t)									
ILLITE + POTASSIUM ACETATE (1:1)										
Initial	54.3	20.0	7.7	1.2	0.0	1.9	1.8	0.0	13.1	---
	Illite (M) Quartz (M) Potassium Acetate (t)									
HTA-Red	54.3	19.3	7.6	1.2	0.0	2.0	1.7	0.0	13.7	---
	Microcline (M) Quartz (M) Cordierite (m) Hematite (t)									
Slag-Red	76.7	15.8	0.7	0.2	0.0	1.6	2.4	0.0	4.6	---
	Amorphous (M)									
ILLITE + MAGNESIUM ACETATE (1:1)										
Initial	54.7	20.3	7.8	1.1	0.1	1.3	8.3	0.0	6.5	---
	Illite (M) Quartz (M) Magnesium Acetate (M)									
HTA-Red	55.8	19.5	7.6	1.2	0.0	1.2	7.5	0.5	6.4	---
	Quartz (M) Akermanite (t) $Ca_3Al_2O_6$ (t)									
Slag-Red	77.0	14.6	0.6	0.2	0.0	1.7	5.8	0.0	0.1	---
	Quartz (M) Amorphous (M)									
ILLITE + SODIUM ACETATE (1:1)										
Initial	56.6	21.0	7.5	1.1	0.0	1.2	2.0	4.3	6.3	---
	Illite (M) Quartz (M) Sodium Acetate (m)									
HTA-Red	56.7	19.9	7.9	1.2	0.1	1.4	1.9	4.6	6.4	---
	N/A									
Slag-Red (N/A)										

KEY: * = SO_3-Free Composition
m = Minor Component
M = Major Component
t = Trace Component

TABLE 5 (CONT.)

MINERAL TRANSFORMATIONS: MODEL MIXTURES

	SiO_2	Al_2O_3	Fe_2O_3	TiO_2	P_2O_5	CaO	MgO	Na_2O	K_2O	SO_3
CALCIUM MONTMORILLONITE + CALCIUM ACETATE (1:1)										
Initial	70.7	15.8	0.9	0.3	0.0	8.8	3.4	0.0	0.0	---
	Quartz (M) Ca-Montmorillonite (M) Calcium Acetate (m) $CaCO_3$ (t)									
HTA-Red	71.3	15.9	0.7	0.3	0.1	8.3	3.3	0.0	0.0	---
	Quartz (M) $Ca(Si,Al)_4O$									
Slag-Red	N/A									
CALCIUM MONTMORILLONITE + MAGNESIUM ACETATE (1:1)										
Initial	72.9	16.4	0.8	0.3	0.1	2.1	6.7	0.7	0.0	---
	Calcium Montmorillonite (M) Quartz (M) Magnesium Acetate (M)									
HTA-Red	72.7	16.2	1.1	0.3	0.0	2.0	7.7	0.0	0.0	---
	Cristobalite (M) Cordierite (M) $MgSiO_3$ (m) Periclase (t)									
Slag-Red	N/A									
CALCIUM MONTMORILLONITE + SODIUM ACETATE (1:1)										
Initial	73.5	16.7	0.8	0.3	0.0	2.1	3.4	3.1	0.0	---
	Calcium Montmorillonite (M) Quartz (M) Sodium Acetate (t)									
HTA-Red	73.5	16.8	0.8	0.3	0.0	2.1	3.4	3.0	0.0	---
	N/A									
Slag-Red	N/A									
CALCIUM MONTMORILLONITE + IRON OXALATE (1:1)										
Initial	69.8	16.0	8.6	0.3	0.0	1.8	3.4	0.0	0.1	---
	Calcium Montmorillonite (M) Iron Oxalate (M) Quartz (M)									
HTA-Red	69.9	15.9	8.4	0.3	0.1	1.9	3.5	0.0	0.1	---
	Cristobalite (M) Mullite (m) Hematite (m)									
Slag-Red	N/A									

KEY: * = SO_3-Free Composition
M = Major Component
m = Minor Component
t = Trace Component
N/A = Not Available

TABLE 5 (CONT.)

MINERAL TRANSFORMATIONS: MODEL MIXTURES

	SiO_2	Al_2O_3	Fe_2O_3	TiO_2	P_2O_5	CaO	MgO	Na_2O	K_2O	SO_3
CALCIUM MONTMORILLONITE + POTASSIUM ACETATE (1:1)										
Initial	71.3	15.9	0.8	0.3	0.0	2.4	3.6	0.0	5.7	---
	Calcium Montmorillonite (M) Potassium Acetate (M) Quartz (M)									
HTA-Red	70.1	15.8	1.4	0.3	0.0	2.6	3.4	0.0	6.4	---
	Cristobalite (M) Spinel (m) $MgSiO_3$ (m)									
Slag-Red	N/A									
SODIUM MONTMORILLONITE + CALCIUM ACETATE (1:1)										
Initial	61.9	18.8	4.5	0.2	0.0	9.2	3.1	1.8	0.5	---
	Sodium Montmorillonite (M) Quartz (m) Calcium Acetate (m)									
HTA-Red	61.5	19.8	5.0	0.2	0.0	8.8	2.8	1.1	0.7	---
	Cristobalite (M) CaO (M) Quartz (m)									
Slag-Red	58.7	22.1	5.0	0.3	0.0	8.4	2.6	2.1	0.7	---
	Amorphous									
SODIUM MONTMORILLONITE + IRON OXALATE (1:1)										
Initial	60.8	18.7	13.4	0.2	0.0	1.8	3.2	1.5	0.6	---
	Sodium Montmorillonite (M) Quartz (M) Iron Oxalate (M)									
HTA-Red	60.4	19.4	13.3	0.2	0.0	2.1	2.9	1.0	0.6	---
	Quartz (M) Hematite (M) FeO Albite (m)									
Slag-Red	58.7	18.7	15.6	0.2	0.0	1.8	2.7	1.4	0.8	---
	Amorphous									
SODIUM MONTMORILLONITE + POTASSIUM ACETATE (1:1)										
Initial	47.1	17.1	4.7	0.3	0.2	2.9	2.3	2.4	22.9	---
	Sodium Montmorillonite (M) Quartz (M) Potassium Acetate (m)									
HTA-Red	51.7	17.3	3.9	0.2	0.1	1.4	2.6	2.2	20.6	---
	$KAlSi_2O_6$ (M)									
Slag-Red	52.7	18.1	3.8	0.2	0.1	2.2	2.7	2.5	17.7	---
	$KAlSi_2O_6$ (M)									

KEY: * = SO_3-Free Composition
M = Major Component
m = Minor Component
t = Trace Component
N/A = Not Available

TABLE 5 (CONT.)

MINERAL TRANSFORMATIONS: MODEL MIXTURES

	SiO_2	Al_2O_3	Fe_2O_3	TiO_2	P_2O_5	CaO	MgO	Na_2O	K_2O	SO_3
SODIUM MONTMORILLONITE + SODIUM ACETATE (1:1)										
Initial	64.0	19.7	4.2	0.2	0.0	1.8	3.5	6.1	0.5	---
	Sodium Montmorillonite (M)			Sodium Hydroxide (M)		Sodium Disilicate (M)				
HTA-Red	63.2	21.0	5.3	0.3	0.0	2.1	3.1	4.1	0.8	---
	Quartz (M)	Albite (M)								
Slag-Red	61.5	21.4	5.7	0.4	0.0	3.0	2.8	4.4	0.8	---
	Amorphous (M)									
SODIUM MONTMORILLONITE + ALUMINUM ACETATE (1:1)										
Initial	55.7	40.1	0.4	2.0	0.0	0.5	1.3	0.0	0.0	---
	Sodium Montmorillonite (M)			Aluminum Acetate (m)						
HTA-Red	60.4	25.1	5.0	0.2	0.0	2.9	3.8	1.9	0.7	---
	Quartz (M)	Cristobalite (M)		Plagioclase (M)		Spinel (m)				
Slag-Red	62.0	25.4	5.1	0.3	0.0	2.1	2.7	1.4	1.0	---
	Mullite (M)									

KEY: * = SO_3-Free Composition
M = Major Component
m = Minor Component
t = Trace Component

calcium acetate to form CaO with subsequent melting of the clay. Gehlenite is not a product of thermal decomposition of kaolinite, but a product of recrystallization of a Ca-rich aluminosilicate melt. The mullite was formed either due to recrystallization from Al_2O_3 and SiO_2-rich melt regions or by decomposition of the kaolinite. The unidentified phase is due presumably to equilibrium not being reached. The slag sample contained anorthite ($CaO.Al_2O_3.2SiO_2$) as a major phase with calcium carbonate observed as a minor phase. The presence of anorthite is consistent with crystallization of the phase from a homogeneous melt. Indeed, equilibrium phase diagrams predict the primary phase of anorthite for this composition, with a liquidus temperature of about 1520°C. The calcium carbonate present is probably due to reaction of residual CaO after exposure.

The chemical composition of all three samples for the kaolinite and magnesium acetate mixture were very similar. The high temperature ash contained mullite and spinel ($MgO.Al_2O_3$) as major crystalline phases with kaolinite observed as a trace phase. These phases are consistent with reaction of the decomposed magnesium acetate with various thermal decomposition products of kaolinite. The mullite is due presumably to decomposition of the kaolinite. As this process produces SiO_2 and not Al_2O_3, the spinel probably formed from a liquid melt phase. The slag contained cordierite ($Mg_2Al_4Si_5O_{18}$) as a major phase; spinel and forsterite (Mg_2SiO_4) were present as minor phases. These phases are consistent with recrystallization of phases from a magnesium-rich homogeneous glass.

The chemical composition of the initial mixture of kaolinite and sodium acetate was slightly different than the high temperature ash and slag. The latter two samples had similar concentrations of all components. The initial mixture, however, had lower SiO_2 and Al_2O_3 than the ash and slag, and higher Fe_2O_3 and Na_2O concentrations. Indeed, the Na/Si molar ratio was calculated to be 1.0 for the initial mixture and only 0.5 for the two treated samples. This shows that there was significant loss of Na with respect to the other components during the ashing process. During the high-temperature ashing, only half the sodium became associated with the aluminosilicate. No further significant loss of sodium was observed during slag formation at 1500°C, indicating that the sodium was in a thermally stable place. X-ray diffraction analysis of the initial mixture showed that there was some quartz and an unidentified phase present. The high-temperature ash contained only corundum (Al_2O_3) and an identified phase, whereas the slag contained only corundum. The corundum is consistent with a process of recrystallization from a homogeneous liquid phase. The unidentified phase is due, presumably, to equilibrium not being attained.

The chemical composition of all three samples of the kaolinite and calcium acetate (1:2) mixture was very similar. The high-temperature ash contained gehlenite ($2CaO.Al_2O_3.SiO_2$) and CaO as major phases, with anorthite ($CaO.Al_2O_3.2SiO_2$) observed as a minor phase. The CaO is derived from the decomposition of the calcium acetate. The gehlenite and anorthite are recrystallization phases from a calcium-rich aluminosilicate glass. The slag contained only anorthite and gehlenite. The equilibrium phase diagram for the $CaO-Al_2O_3-SiO_2$ system would predict for the slag composition a liquidus temperature of 1650°C with a primary crystalline phase of gehlenite. The two phases observed probably formed during the slow cooling of the glass in the furnace before removal.

The initial chemical composition of the kaolinite, sodium acetate, and quartz (1:1:2) model mixture had slightly lower levels of SiO_2 and Al_2O_3 than the ash and slag samples, and a higher Na_2O level. Calculation of the Na/Si molar ratio for each of the samples showed that there was significant loss of Na with respect to the major component. The Na/Si ratio for the initial mixture was 0.4, whereas the ash and slag had a ratio of about 0.2. This is similar to the loss of Na observed with the kaolinite sodium acetate (1:1) mixture. X-ray diffraction analysis of the high-temperature ash showed nepheline ($NaAlSiO_4$) and quartz to be present as major phases. The nepheline is a product of recrystallization from a melt phase, whereas the quartz is a residual phase. Phase equilibria for the system Na_2O-Al_2O_3-SiO_2 shows a eutectic phase at about 730°C for the composition, with a liquidus of about 1100°C. The primary crystalline phase would be corundum (Al_2O_3) for the composition. However, the unmelted quartz observed in the ash would push the composition of the melt into the nepheline primary phase. The observance of corundum in the slag corresponds to that expected from the phase diagram for the system with only a minor amount of residual quartz present.

The chemical composition of the initial mixture of kaolinite, potassium acetate, and quartz showed less SiO_2 and more K_2O than the high-temperature ash and slag samples. The slag sample had higher SiO_2 and lower Al_2O_3 than the other samples. Calculation of the K/Si molar ratio showed that the initial mixture had a ratio of 0.4 and 0.3, respectively. This indicates that K was volatilized only at the high temperatures reached during slag formation. This behavior contrasts markedly with the corresponding mixture with sodium acetate where significant amounts of sodium were volatilized during high-temperature ashing. The x-ray diffraction analysis showed that quartz was observed as a major phase in the high-temperature ash with $Ca_3Al_{10}O_{18}$ as a minor phase. Careful analysis of the x-ray diffraction pattern, however, showed that there was significant amorphous phase present. The quartz, of course, was a residual phase, while the $Ca_3Al_{10}O_{18}$ was probably due to heterogeneity of the sample. The slag sample contained leucite ($KAlSi_2O_6$) and quartz as major phases with corundum observed as a minor phase. The leucite and corundum are the expected crystalline phases formed from a potassium-rich aluminosilicate glass, based on phase equilibrium diagram for the system K_2O-Al_2O_3-SiO_2.

The analysis of the mixture kaolinite iron oxalate and quartz (1:1:1) had not been completed at the time of this report.

The chemical composition of the initial mixture of kaolinite, magnesium acetate, and quartz (1:1:1) was identical to the chemical composition of the high-temperature ash. However, the slag sample had higher SiO_2 and lower Al_2O_3 and MgO contents than the other samples. Comparison of the Mg/Si molar ratio showed that the initial samples and high-temperature ash had a value of 0.4. This was higher than that calculated for the slag sample (0.3). The results indicate that there was some loss of Mg from the system with respect to the SiO_2 content during slag formation. In terms of crystalline phase assemblage, the high-temperature ash contained quartz, spinel ($MgO.Al_2O_3$), and mullite ($3Al_2O_3.2SiO_2$) as major phases. The presence of mullite and spinel are consistent with limited reaction between the kaolinite and magnesium oxide (from decomposition of the acetate) to a magnesium-rich aluminosilicate glass. The quartz was a residual phase from the initial mixture. The slag for this mixture contained only indialite ($2MgO.2Al_2O_3.5SiO_2$). Indialite is a

high temperature polymorph of cordierite. The composition of the slag when plotted on the phase diagram of the system $MgO-Al_2O_3-SiO_2$ showed a primary phase of cordierite (the equilibrium phase) with a liquidus temperature of about 1500°C. This indicates that the slag approached thermal equilibrium.

The analysis of the mixture illite and calcium acetate had not been completed at the time of this report.

The chemical composition of the initial mixture of illite and iron oxalate was very similar to the high-temperature ash. However, the slag sample had higher SiO_2, Al_2O_3, and MgO and much lower Fe_2O_3 and K_2O levels than the initial mixture and high-temperature ash. Calculation of the Fe/Si and K/Si molar ratios showed that there was significant loss of Fe and K from the system during slag formation. X-ray diffraction analysis of the initial mixture revealed some quartz present, which is presumably an impurity of the illite clay. The high-temperature ash contained crystalline quartz and hematite as major phases. These phases are consistent with complete melting of the clay and decomposition followed by oxidation of unreacted iron oxalate. The x-ray diffraction analysis of the slag showed a large amorphous peak with a trace of hematite. This indicates that all reactants melted, except for some residual hematite, to form a glass.

The chemical composition of the initial mixture of illite and potassium acetate (1:1) was almost identical to that of the high-temperature ash. The slag, however, had higher SiO_2 and lower Al_2O_3, FeO, and K_2O contents. Indeed, there appeared to be negligible Fe_2O_3 present in the slag and the K/Si molar ratio decreased from 0.3 to 0.1. This indicates that all the potassium added as acetate is lost due to volatilization during slag formation. The high-temperature ash contained microcline and quartz as major phases with cordierite and hematite observed as minor and trace phases, respectively. The microcline and cordierite were formed probably due to recrystallization from a potassium-rich and a magnesium-rich liquid phase, respectively. The low MgO level in the bulk chemical composition suggests that the sample was quite heterogeneous. The quartz and hematite observed is due to thermal decomposition, and the quartz is a residual phase. The slag did not exhibit any crystalline phases, indicating that the sample was amorphous.

The chemical composition of the initial mixture of illite and magnesium acetate was very similar to that of the high-temperature ash. The slag sample had a much higher SiO_2 and very low Fe_2O_3 and K_2O levels than the other samples. The loss of K_2O was more marked than that observed formed from the illite and potassium acetate mixture. X-ray diffraction analysis of the high-temperature ash showed quartz as a major phase with akermanite ($2CaO.MgO.2SiO_2$) and $Ca_3Al_2O_6$ observed as trace phases. Akermanite and $Ca_3Al_2O_6$ are products of recrystallization from a melt. This indicates significant melting. However, the low CaO content of the sample and the fact that $Ca_3Al_2O_6$ is not an equilibrium phase below about 1335°C (based on the phase equilibria system $CaO-Al_2-SiO_2$) suggested that the melt phase was not homogeneous. The slag contained quartz only, indicating incomplete melting. However, the clay and magnesium acetate appeared to have reacted and melted.

As shown previously in Table 5, the analysis of the mixtures illite + sodium acetate, calcium montmorillonite + magnesium acetate, calcium

montmorillonite + sodium acetate, calcium montmorillonite + iron oxalate, and calcium montmorillonite + potassium acetate have not been completed at this time.

The chemical composition of the initial sodium montmorillonite and calcium acetate mixture was very similar to that of the high-temperature ash. The slag sample, however, had lower SiO_2 and higher Al_2O_3 levels than the other samples. Unlike the other samples with calcium acetate additions, there was no relative loss of CaO with respect to the other components. The x-ray diffraction analysis of the initial mixture showed some contamination of quartz in the clay sample. The high-temperature ash contained cristobalite (high-temperature polymorph of SiO_2) and CaO as major phases, with quartz present as a minor phase. The phases are consistent with decomposition of the clay and calcium acetate. As no crystalline phase was observed which contained Al_2O_3 and components other than SiO_2 and CaO, these components must have been present in the amorphous phase. The slag did not exhibit any crystalline phases.

The chemical composition of the initial mixture of sodium montmorillonite and iron oxalate was very similar to that of the high-temperature ash. The chemical composition of the slag was also similar. The only difference to note is the slightly higher Fe_2O_3 and lower SiO_2 contents of the slag compared to the other samples. X-ray diffraction analysis of the high-temperature ash showed that quartz and hematite were present as major phases, with iron (II) oxide and albite ($NaAlSi_3O_8$) observed as minor phases. The quartz was a residual phase, while the hematite and iron (II) oxide were formed by thermal decomposition of the iron oxalate under reducing conditions. The albite is a product of recrystallization from a sodium-rich aluminosilicate glass. The presence of albite in a sample with very low Na_2O on a bulk basis suggests that the sample was heterogeneous. The slag sample was shown by x-ray diffraction to be amorphous.

The chemical composition of the initial mixture of sodium montmorillonite and potassium acetate had lower SiO_2 and higher K_2O than the high-temperature ash and slag. Both the high-temperature ash and slags had similar chemical composition. The major difference was the lower K_2O content of the slag compared to the ash. Calculation of the K/Si molar ratio for all three samples showed a decrease in the value from 0.6 for the initial mixture to 0.5 and 0.4 for the ash and slag, respectively. Though the loss of potassium was significant, it does not appear to be as great as that observed with the illite mixtures. X-ray diffraction analysis revealed that only leucite ($KAlSi_2O_6$) was present in the high-temperature ash and slag samples. Leucite is the crystalline phase expected for the compositions based on the equilibrium system K_2O-Al_2O_3-SiO_2.

The analysis for the mixture sodium montmorillonite and magnesium acetate has not been completed to date.

The chemical composition of the initial mixture sodium montmorillonite and sodium acetate was similar to the high-temperature ash. The ash, however, had slightly higher Al_2O_3, Fe_2O_3, CaO, and K_2O levels than the initial composition and lower Na_2O. The slag formed from the high-temperature ash had slightly less SiO_2 and slightly more CaO than the ash. The Na/Si molar ratio for the initial mixture was 0.18, which was greater than that for the ash and

slag (0.13 and 0.14). As the Na/Si molar ratio in the sodium montmorillonite is about 0.10-0.13, the sodium lost from the mixture appears to be from the acetate and not the mineral phase. X-ray diffraction of the initial mixture showed that the sample contained sodium montmorillonite, sodium hydroxide, and sodium disilicate as major phases. No sodium acetate was observed. The sample was prepared for a second time under carefully controlled conditions and the same phases were observed. Indeed, a distinct color change was observed during mixing. The high-temperature ash contained quartz and albite ($NaAlSi_3O_8$) as major crystalline phases. The quartz is a residual mineral phase. Albite was formed as a recrystalline phase. Indeed, the phase would be predicted by the phase diagram of the system Na_2O-Al_2O_3-SiO_2 for the bulk chemical composition. The slag was amorphous, which would also be expected from the phase diagram. The composition lies in the albite primary phase field and has a liquidus temperature of about 1100°C.

The chemical composition of the initial mixture of sodium montmorillonite and aluminum acetate was very different than the high-temperature ash and the slag. The initial mixture had lower SiO_2 and higher Al_2O_3 levels than the ash and slag samples. The mixture also had very low Fe_2O_3, CaO, MgO, Na_2O, and K_2O compared to the ash and slag. The ash and slag samples had very similar chemical compositions. Comparison of the Al/Si molar ratio shows that nearly all the Al added as acetate is volatilized during ashing. X-ray diffraction analysis of the ash showed that the sample contained quartz, cristobalite, and plagioclase ($CaO.Al_2O_3.2SiO_2$) as major phases, with spinel observed as a minor phase. The plagioclase and spinel are formed by recrystallization from Ca- and Mg-rich aluminosilicate melts. Their presence, as well as that of quartz, indicates that the sample had not reached equilibrium. The slag sample contained mullite only. This phase would be expected from the composition on the SiO_2-Al_2O_3 phase diagram.

The results of the mineral transformation studies require extensive analysis before significant conclusions can be reached. However, interesting features have been observed, such as the volatilization of potassium in illite-based slags and the low-temperature melting of sodium montmorillonite clay mixtures.

4.2 Task B. Volatilization Studies

The pressure pyrolysis unit was used to prepare chars from the test coals under carefully controlled conditions. The char samples obtained have been submitted for analysis. The six coals, Wyodak, Martin Lake, Velva, Indian Head, Illinois No.6, and Pittsburgh No.8, will be subjected to pressure pyrolysis at 850°C under pressures of 14.7, 200, and 400 psi to determine the effect of pressure on mineral transformations and volatilization of inorganic components. The pyrolysis was run under 10% H_2-90% N_2 gas to simulate the reducing conditions of coal gasification. In order to obtain enough material for analysis, two duplicate runs are required. Runs completed to date are shown on the following page.

Coal	Pressure (psi)	Temperature (°C)	Runs Completed
Wyodak	14.7	850	1/2
Martin Lake	14.7	850	1/2
Illinois No.6	14.7	850	1/2
Indian Head	none completed		0
Velva	14.7	850	2/2
Velva	200	850	2/2
Pittsburgh No.8	14.7	850	2/2
Pittsburgh No.8	200	850	2/2

Proximate analysis of the chars have shown that the percent fixed carbon and volatiles were within the expected range of the values which should be obtained from chars produced during mild gasification conditions (12).

Improvements to the pressure pyrolysis unit have been identified. These improvements include new methods for obtaining a complete mass balance and design modifications to allow larger quantities of sample to be processed. Another possible improvement is redesign of the unit to allow the sample to be introduced to the reactor at run temperature.

To obtain a better mass balance, liquid and vapor collection was performed in the unit using a liquid nitrogen-cooled trap filled with glass beads. Most of the tars condensed before reaching the trap and vapors collected on the glass beads in the form of a thin film. A suitable method for collecting the trapped volatiles from the glass beads and analyzing them on both a qualitative and quantitative basis is under consideration. Another problem affecting the mass balance is that some coal is blown out of the crucibles during the run. Design for a larger reactor and sample input modifications will be considered after the present test matrix is completed.

A copy of the PACKAGE code was supplied by Dr. Nagarajan of METC. Significant effort was made to install the code on both UND mainframe computers. Successful installation was achieved on the Microvax computer system in the School of Engineering and Mines. The code, written in Fortran, involves data input and output through tape devices. The University system uses disk drives and therefore changes in the program must be made in order to run the code successfully at UND. The PACKAGE code logic manual has just been acquired, which should aid in making the required changes and assist in the operation of the code.

Initial attempts to expand a SOLGASMIX data base to include carbon were unsuccessful. This was due to the limit of ten elements in the pc version of the program developed at Penn State. However, the mainframe SOLGASMIX program is expandable to include up to 20 elements. A copy of the mainframe code will be obtained in the near future and installed.

Enthalpy and entropy data for liquid and solid calcium sulfate was calculated and added to the database. The composition of the Wyodak char produced at ambient pressure and 850°C was used in SOLGASMIX to predict the behavior of the inorganic components and phases of the char over a range of temperatures. The total moles of elements in the char were obtained from proximate analysis of the char and the composition of the ash was determined from SEMPC analysis of the char (in the absence of other data such as ultimate analysis or chemical fractionation). The moles of reducing gas were based on

the temperature and volume of the reactor. The results showed that the relative quantities of the predicted components were consistent with the elemental quantities entered into SOLGASMIX. Verification of the SOLGASMIX predictions will be accomplished by comparing them with the phases observed from mineral transformation studies (Task A). A significant result in the pressure pyrolysis of Wyodak char at ambient pressure and 850°C was the loss of appreciable fractions of Ca and Mg. Tables 6 and 7 compare the proximate analysis and chemical composition of the reduced HTA with the chemical composition of the char determined by SEMPC. The data shows that the ash formed during pyrolysis can be very different chemically, and possibly mineralogically, than the ash produced under reducing conditions (longer residence time). The same Wyodak char composition will be used in the atmosphere on SOLGASMIX predictions. SOLGASMIX will be used to predict the composition of the chars and ashes of the six test matrix coals. The data will be used to determine the chemical composition and relative amount of phases (gas, liquid, and solid).

The data required for input into the PC SOLGASMIX is an initial composition which can be of the coal, char, or ash. It is critical to determine the best input source because it will affect the output phase assemblage. ASTM ash was not chosen as the input stream because it is produced under oxidizing conditions representative of combustion systems and not under conditions representative of gasifier systems. A coal basis was not chosen for modeling of gasifier conditions for the following reasons. Gasification is essentially two steps, pyrolysis (loss of volatiles) and gasification of the pyriolyzed char. If a coal basis was used, SOLGASMIX would be required to first predict the volatiles lost, then predict the phases and components of the remaining species. Therefore, the char best represents a basis for gasifier systems. Chars produced under pressure pyrolysis conditions (10% hydrogen, 90% nitrogen) will be used as input for SOLGASMIX. The data will be compared with that predicted, using SOLGASMIX, from the chemical composition of the coal and the ash produced under oxidizing conditions. This comparison will show the difference in phase assemblages that would occur with the different compositions under gasifier conditions. In the future, it will be important to be able to model the char composition from standard coal analyses in order to properly predict the ash behavior in the gasifier. When mineral transformation data is more complete, the coal or ash composition will be the most practical for industrial use.

Wyodak char produced at 850°C and ambient pressure was chosen as a first test case. SOLGASMIX was used to predict the phases (gas, liquid, and solid) present over a range of temperatures between 700° and 1750°C. For the Wyodak char, reducing gases were considered as components in the initial composition. Generally, SOLGASMIX predicted phases similar to those observed in coal ash systems. For example, albite ($NaAlSi_3O_8$), iron oxide, and SiO_2 were detected in the char using SEMPC and were correctly predicted using SOLGASMIX. However, phases were observed, such as iron sulfide and anhydrite, which were not predicted by SOLGASMIX at the temperature at which the char was produced. This is probably due to the fact that the char had not reached equilibrium and that the char matrix prevented the diffusion of components to form the reaction products. SOLGASMIX, on the other hand, predicted phases which are generally not observed in coal ash products; for example, calcium leucite, corundum (Al_2O_3), and magnesium silicate. These phases are not common to coal ash systems. The results show that detailed evaluation of

TABLE 6

COMPARISON OF PROXIMATE ANALYSIS OF WYODAK CHAR WITH RAW COAL

Wyodak Coal (Wt%)		Wyodak Char (Wt%)	
Moisture	18.98	Moisture	0.56
Volatiles	34.07	Volatiles	4.19
Fixed Carbon	40.21	Fixed Carbon	64.01
Ash	6.72	Ash	31.22

TABLE 7

COMPARISON OF CHEMICAL COMPOSITION OF WYODAK CHAR WITH HTA'S

	Elemental Wt%				
Wyodak Char (SEMPC)*		Wyodak Red Ash (XRFA)		Wyodak Ox Ash (XRFA)	
Si	26.4	Si	16.4	Si	13.2
Al	7.3	Al	8.4	Al	9.6
Fe	7.2	Fe	2.5	Fe	2.6
Ti	0.2	Ti	1.0	Ti	1.1
P2	0.2	P	0.5	P	0.7
Ca	2.9	Ca	16.5	Ca	16.5
Mg	0.4	Mg	3.2	Mg	4.3
Na	0.8	Na	0.6	Na	0.7
K	1.7	K	0.3	K	0.3
S	4.3	S	3.9	S	4.6
O+	48.6	O+	46.7	O+	46.4

* Chemical composition determined from average of all points analyzed in SEMPC routine.

+ Oxygen by difference.

SOLGASMIX is necessary in order for the technique to become a valuable tool in the modeling of coal ash behavior in gasification systems. The use of a larger SOLGASMIX program will allow the inclusion of more elements, and hence more phases, which should improve the predicted equilibrium phase assemblage. Furthermore, knowledge of the phases which are common to coal ash systems will allow preclusion of erroneous phases. This will provide more accurate predictions of the behavior in gasification systems.

4.3 Task C. Viscosity Studies

The viscosity/temperature curves have been determined for all of the coal ash samples (both oxidized and reduced ash). The viscosity was measured under reducing atmosphere (8% hydrogen, 92% nitrogen). Figures 5 through 10 show the viscosity curves for both the oxidized and the reduced ash for each of the coal samples.

In general, the reduced ashes tended to exhibit a lower viscosity at a given temperature than the corresponding oxidized ash. The exceptions to this observation are the results for Illinois No.6 and Wyodak. In both cases, the reduced ash slag had a much higher Si/Al molar ratio than the oxidized ash slag. The viscosity temperature curves for both types of ashes (oxidizing and reducing) tended to have similar profiles. The low-rank coal ashes, however, showed marked deviation at lower temperature. The most extreme example was observed for Velva coal, where the oxidized ash had a much higher viscosity at temperatures below 1410°C than the reduced ash. Indian Head and Martin Lake ashes also showed differences in their viscosity/temperature profiles. The different profiles observed are due, presumably, to differences in crystallization behavior or chemical composition between the ash samples.

An extensive viscosity/temperature data base was developed after a detailed review of the literature. The database contains almost 2,000 data pairs and covers viscosity of simple oxide glasses, geological slags, and coal ash slags. This data base was compiled in order to develop a viscosity model which covered all ranks of coals, as well as the wide range of component liquid phases responsible for sintering in ash systems. The approach used in the development of the model was to fit viscosity data of simple oxide glasses (the extensive data of Machin et al. on the system $CaO-MgO-Al_2O_3-SiO_2$) to a general model of viscosity. Based on previous experience at UNDEMRC, the model developed by Urbain et al was chosen as a starting point. Using the data for simple oxide glasses, corrections in certain coefficients in the Urbain model were made. The resulting model, called the corrected Urbain, was then tested with the extensive coal ash database of Watt and Fereday (3). Figure 11 shows the comparison of measured viscosity versus calculated viscosity for 334 data sets for the Watt and Fereday data. The viscosities were measured over the temperature range 1200° to 1500°C. A linear regression of the curve gave an excellent fit with an r^2 of 0.92, gradient of 1.30, and a constant of -23. The model was tested against the NBS glass standard used to calibrate the viscometer. The model gave excellent fit over the experimental temperature range (Figure 12) and the predictions were well within the acceptable range for the glass.

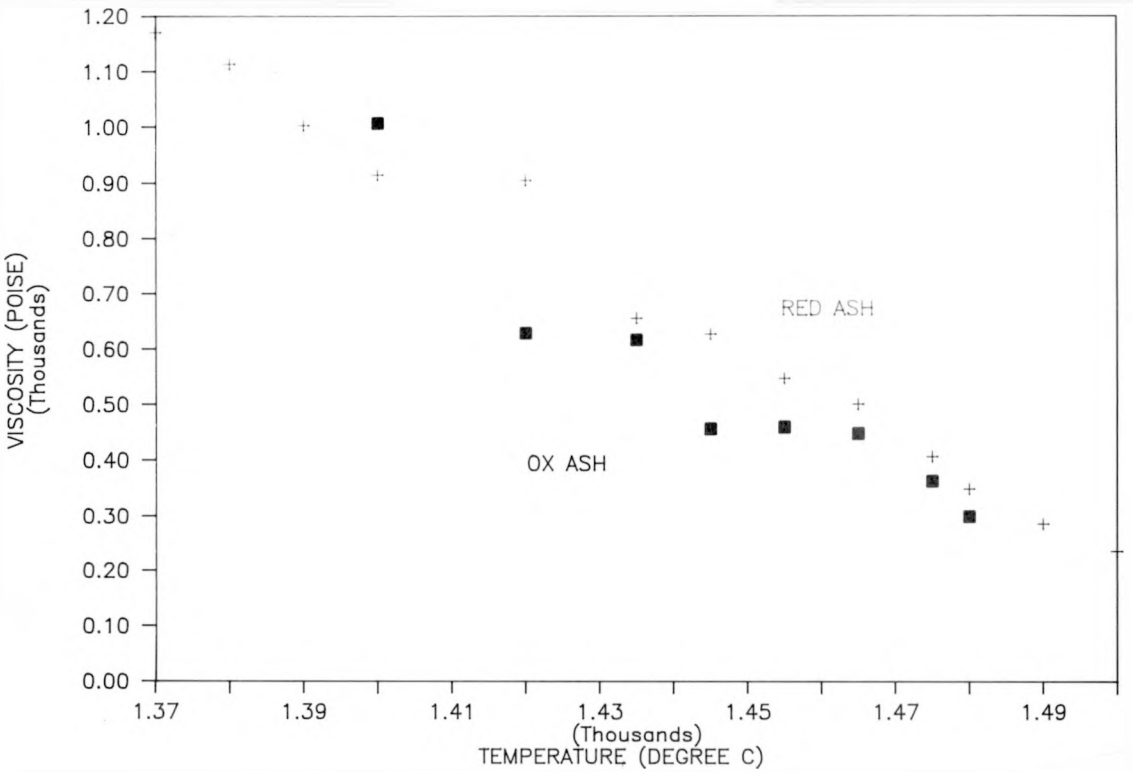

Figure 5. Viscosity/Temperature Data for Illinois No.6 Coal Ash (reduced and oxidized ash) Measured under Reducing Atmosphere

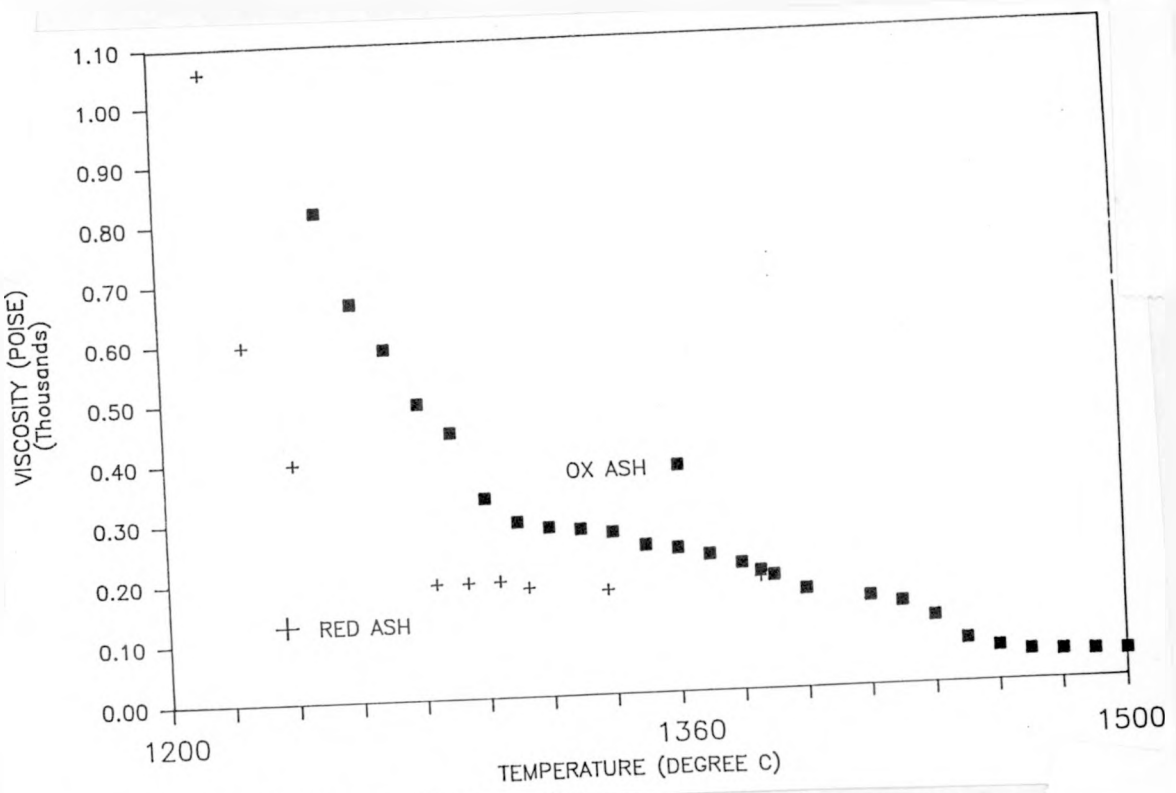

Figure 6. Viscosity/Temperature Data for Indian Head Coal Ash (reduced and oxidized ash) Measured under Reducing Atmosphere

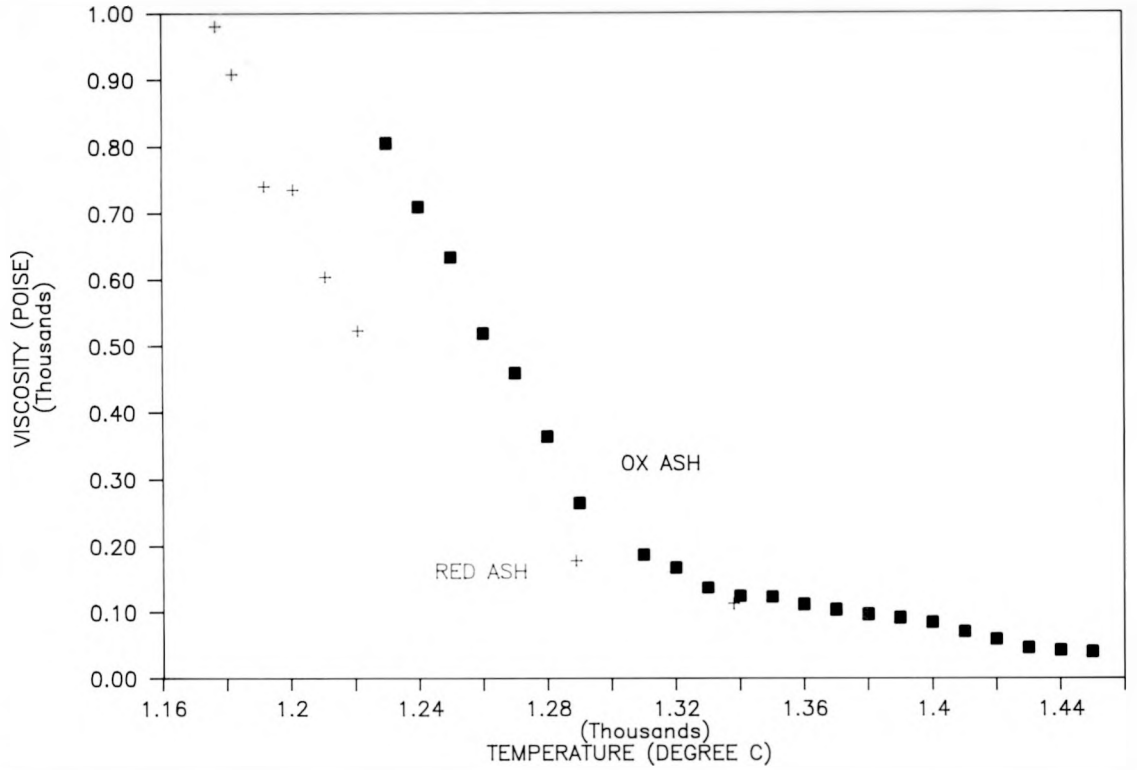

Figure 7. Viscosity/Temperature Data for Martin Lake Coal Ash (reduced and oxidized ash) Measured under Reducing Atmosphere

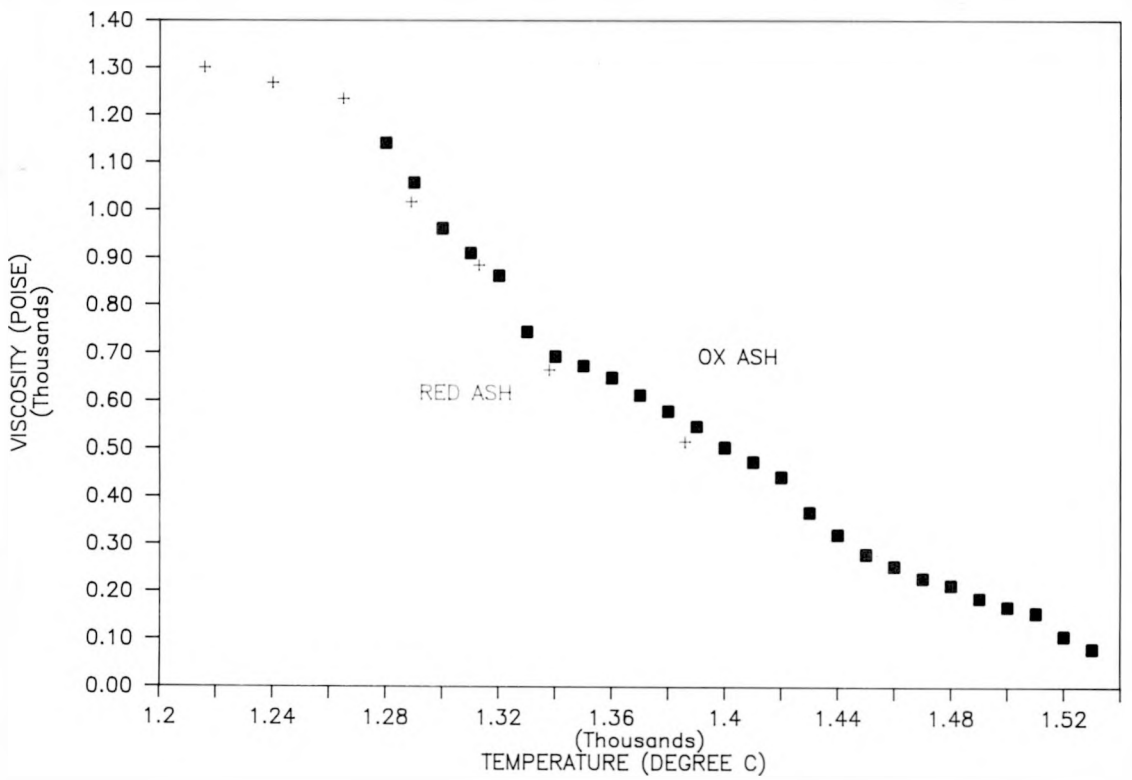

Figure 8. Viscosity/Temperature data for Pittsburgh No.8 Coal Ash (reduced and oxidized ash) Measured under Reducing Atmosphere

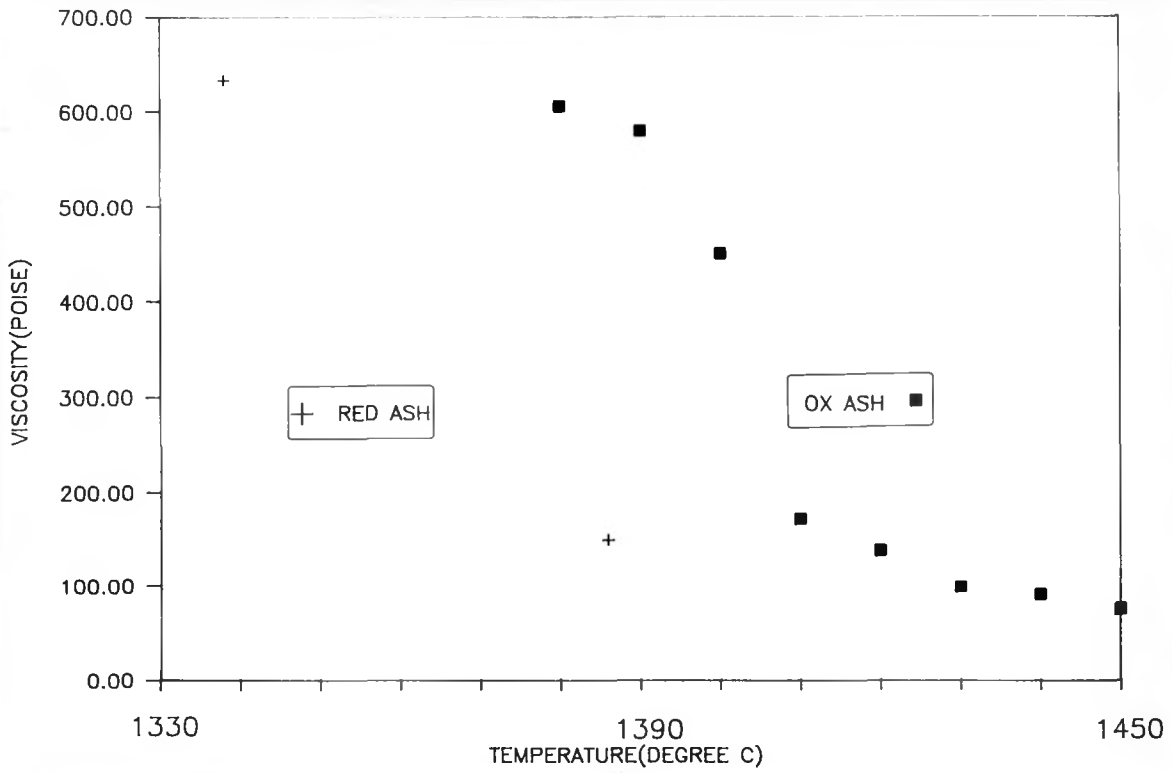

Figure 9. Viscosity/Temperature Data for Velva Coal Ash (reduced and oxidized ash) Measured under Reducing Atmosphere

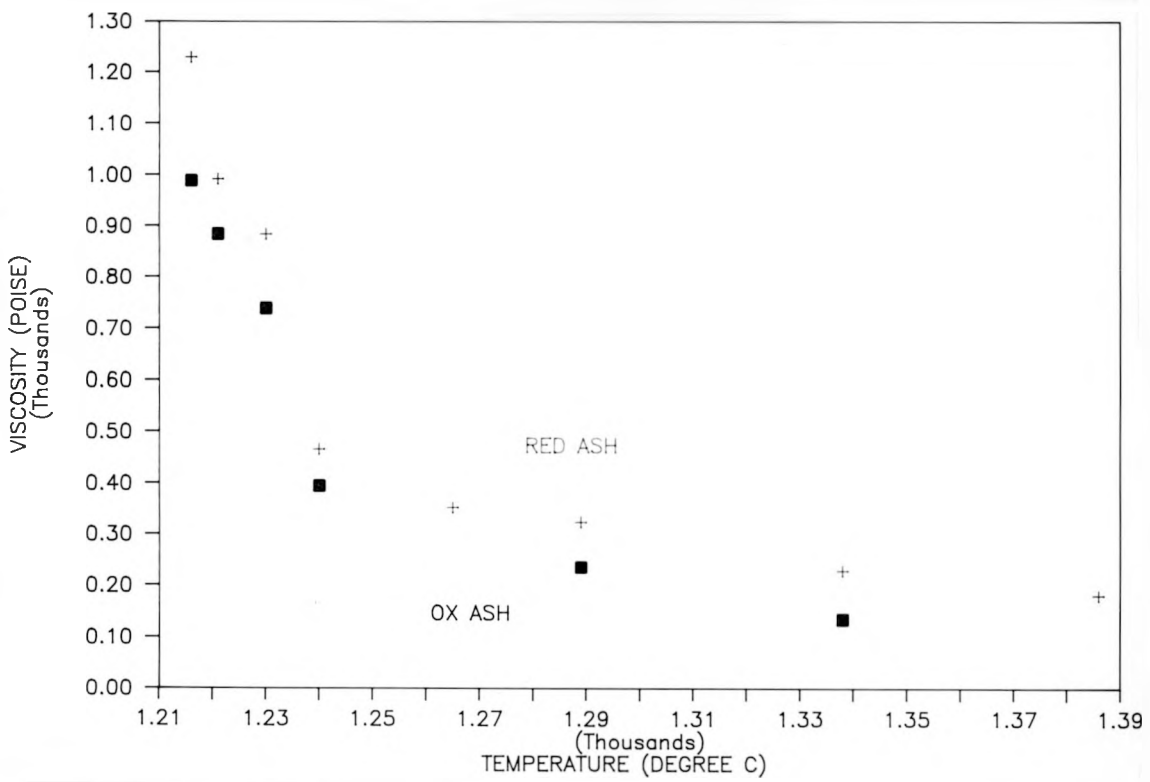

Figure 10. Viscosity/Temperature Data for Wyodak Coal Ash (reduced and oxidized ash) Measured under Reducing Atmosphere

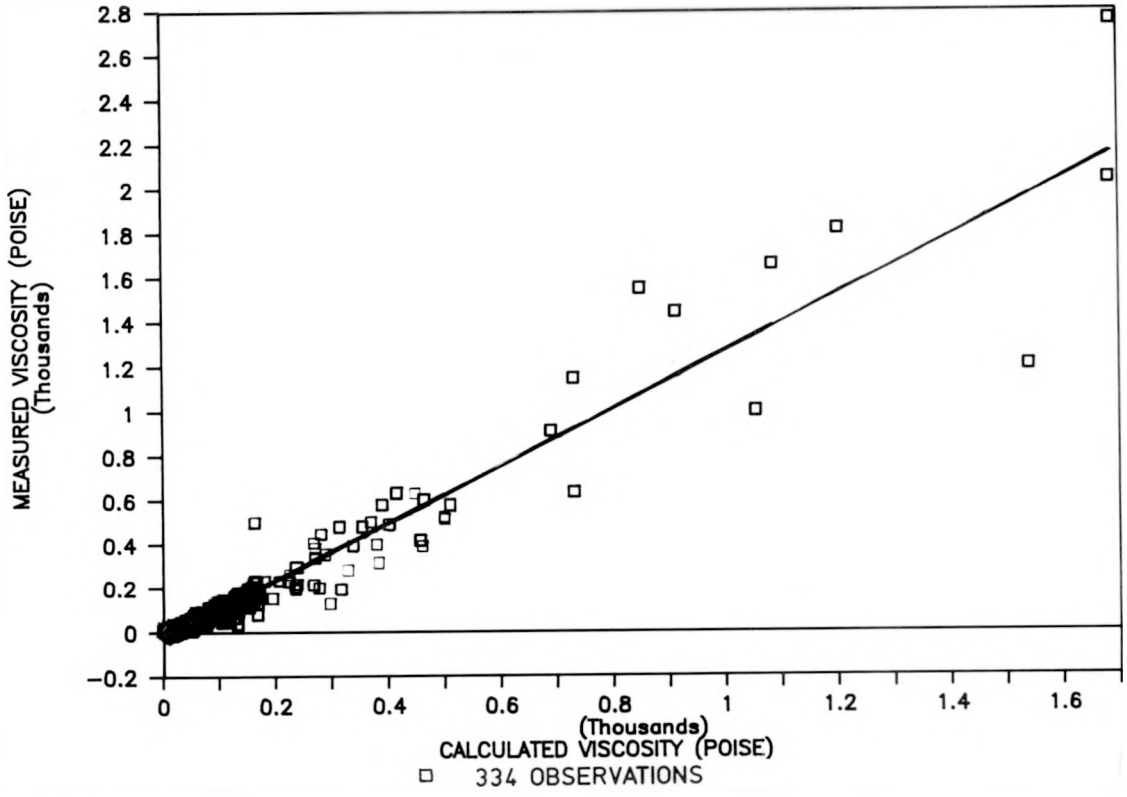

Figure 11. Measured Viscosity Versus Calculated Viscosity Using the Corrected Urbain Model (data of Watt and Fereday)

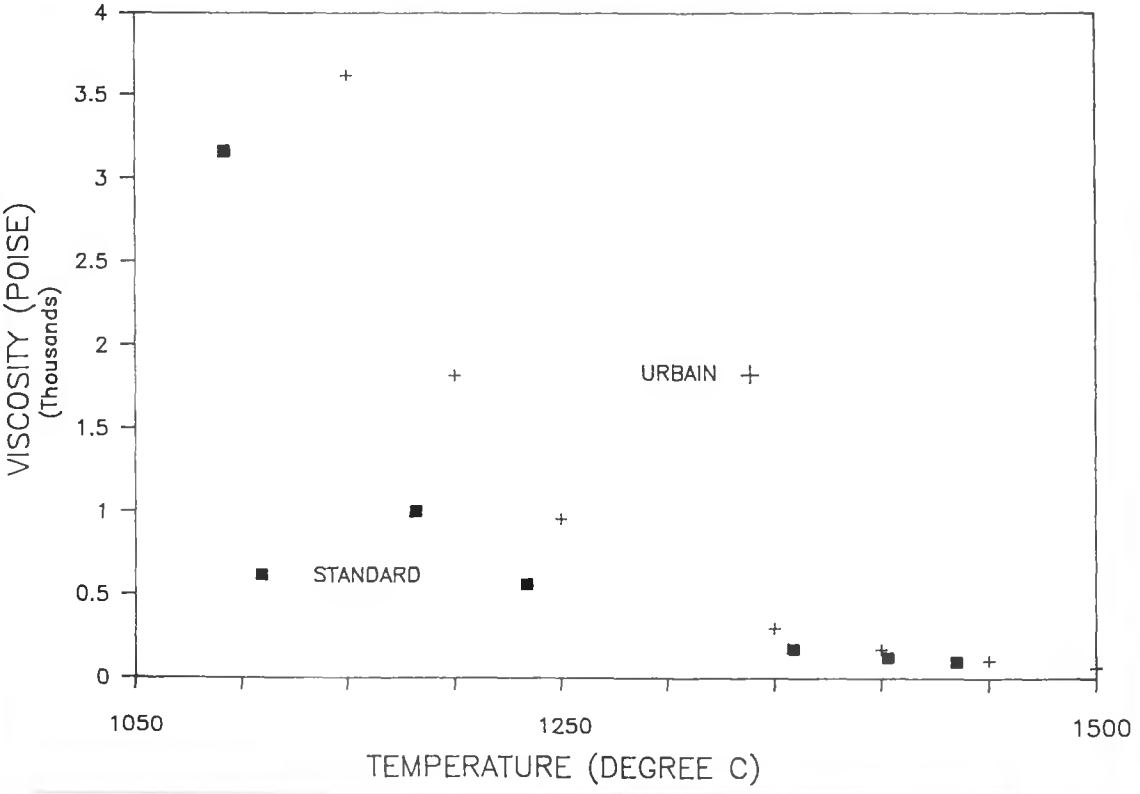

Figure 12. Viscosity/Temperature Curve for NBS glass standard Compared With Predicted Viscosity Based on Corrected Urbain

The corrected Urbain model was used to predict the viscosity of slags studied in this project. Figures 13 through 18 are the viscosity temperature curves for each of the reduced coal ash samples studied. Included in each figure are the predictions based on the uncorrected Urbain, the corrected Urbain, the corrected Urbain using the SO_3-free composition, and the four major components.

The corrected Urbain gave excellent fit with the measured viscosities for Illinois No.6 (Figure 13). The worst fit was observed for the original Urbain model. In the case of Indian Head (Figure 14), the best fit was observed with the corrected Urbain using the four major components (SiO_2, Al_2O_3, Fe_2O_3, and CaO).

The four major components in the corrected Urbain model gave better fit to the measured values for Martin Lake (Figure 15). Below 1300°C, a steep rise in viscosity was observed. This was due, presumably, to crystallization of the sample. In the case of Pittsburgh No.8, the SO_3-free corrected Urbain model gave the best fit (Figure 16). The corrected and original Urbain gave good fit down to about 1310°C. For the Velva coal (Figure 17), none of the models fit the experimental results below 1450°C. Characterization of the slags, as reported above, showed extensive crystallization. The crystallization, caused by a high liquidus temperature, may be the reason for the discrepancy between measured and predicted viscosity. In the case of the Wyodak coal (Figure 18), the original Urbain fit the experimental results at high temperatures (above 1300°C), while the corrected Urbain gave excellent fit to the data at lower temperatures.

The corrected Urbain model, in general, gives excellent fit to the experimental results for the coal ashes over the Newtonian fluid range. The model can be used to predict bulk flow properties, as well as the flow of component liquid phases which participate in the sintering and agglomeration behavior of ashes.

4.4 Task D. Surface Tension

The surface tension data for all of the coal ash studies has been compiled. The data is listed in Table 8. The data for sodium montmorillonite is also included. In general, the reduced coal ash exhibited a lower surface tension than the oxidized coal ash. The exception to this was the Velva sample. Detailed correlations of chemical composition to surface tension will be attempted in the near future.

The compilation of a database for surface tension of aluminosilicate melts and coal ashes has been initiated. The data base, to date, includes the results of this study and the data of Kozakevitch (13). When completed, the data base will be used to determine the relationship between chemical composition, atmosphere, temperature, and surface tension of a molten ash species in gasifiers.

4.5 Related Task

The results of this study have been applied to the formation and behavior of ash in actual pilot-scale and full-scale gasifiers. gasifiers. General results of the study of agglomeration and clinkering in a coal gasification system are described in the Appendix.

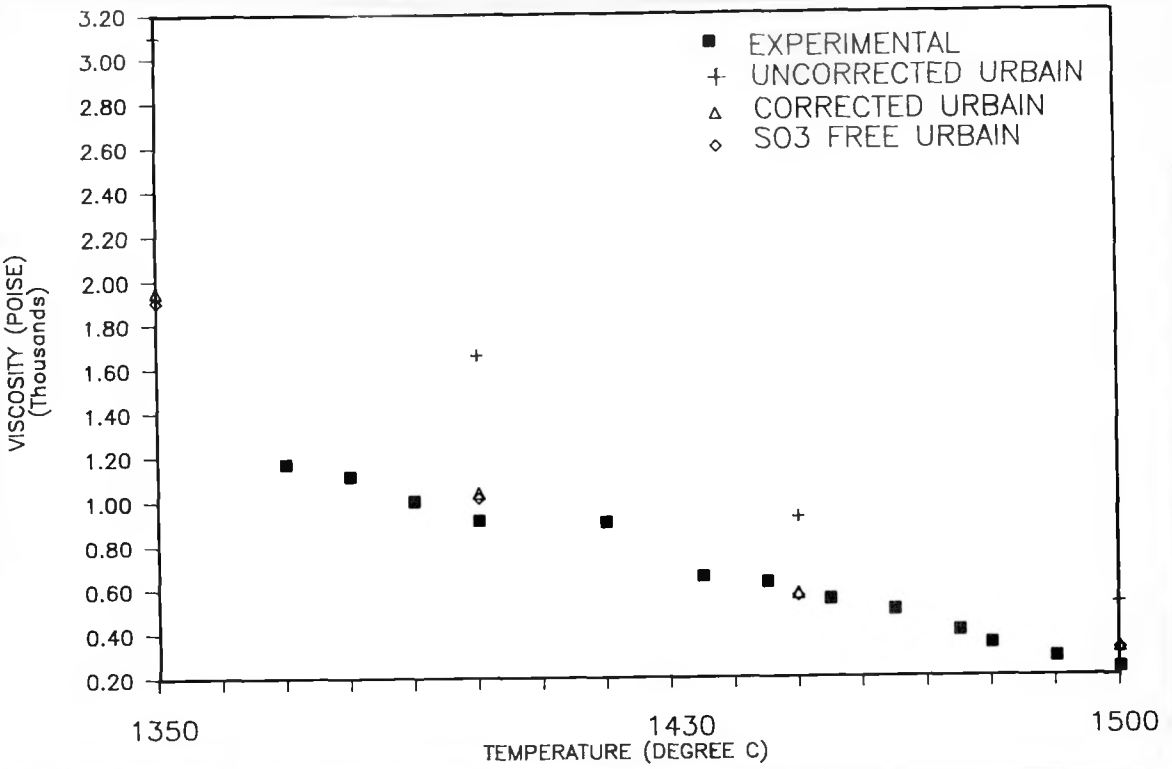

Figure 13. Comparison of Measured Viscosity With Various Models of Viscosity for Illinois No.6 Coal (reducing atmosphere from reduced ash)

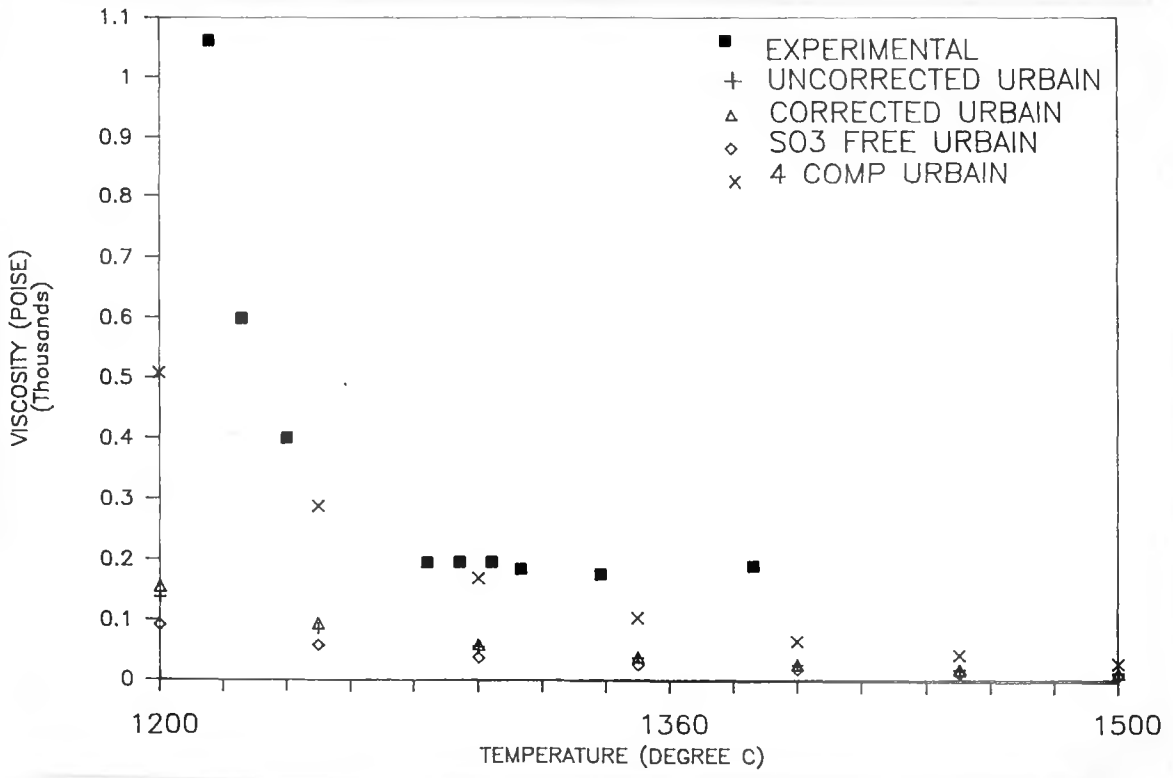

Figure 14. Comparison of Measured Viscosity With Various Models of Viscosity for Indian Head Coal (reducing atmosphere from reduced ash)

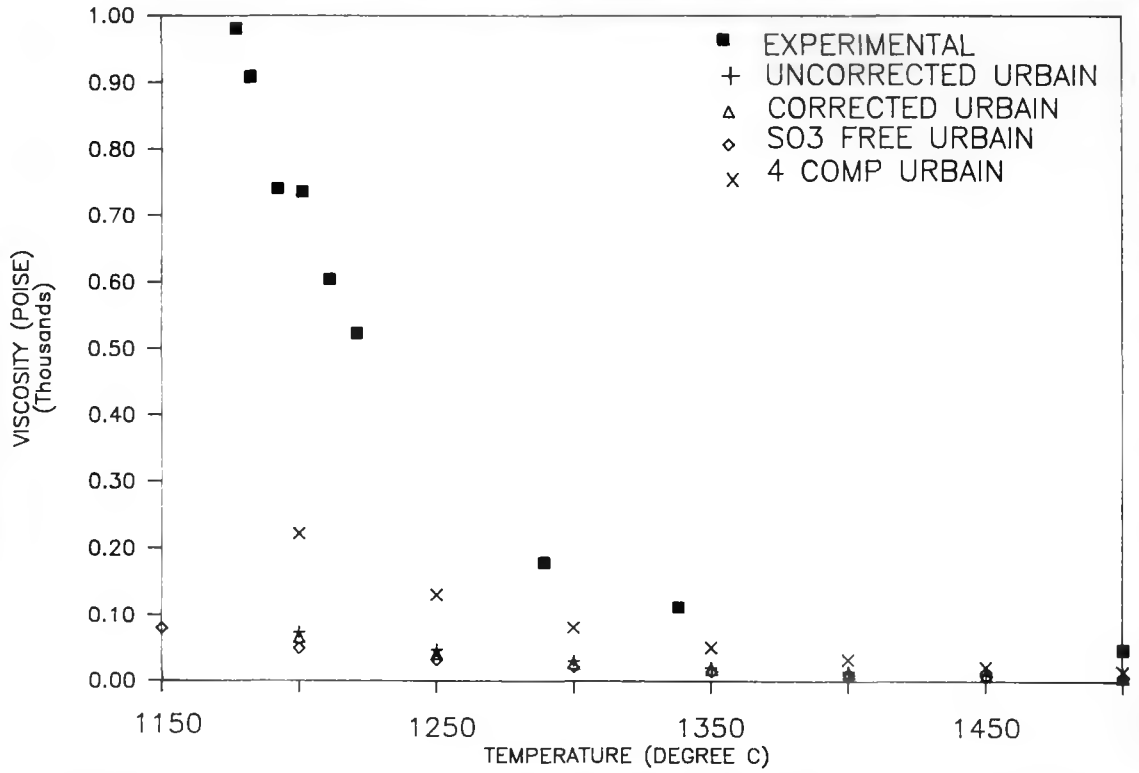

Figure 15. Comparison of Measured Viscosity With Various Models of Viscosity for Martin Lake Coal (reducing atmosphere from reduced ash)

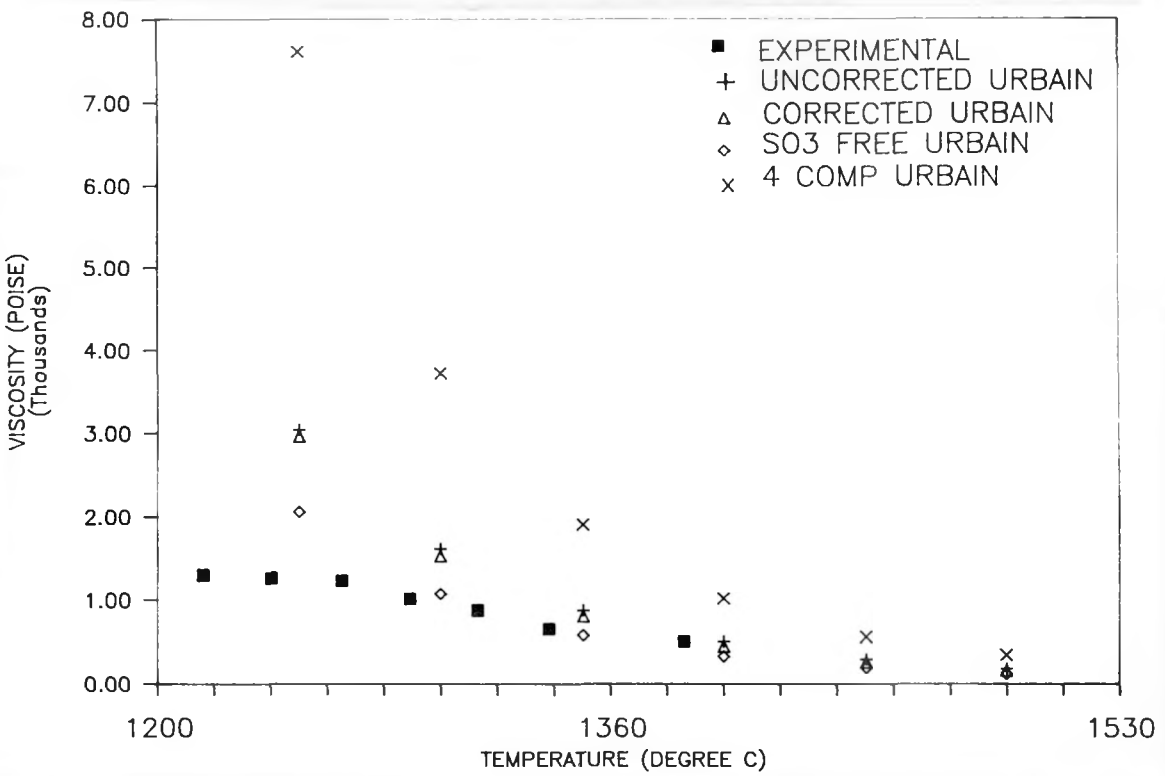

Figure 16. Comparison of Measured Viscosity With Various Models of Viscosity for Pittsburgh No.8 Coal (reducing atmosphere from reduced ash)

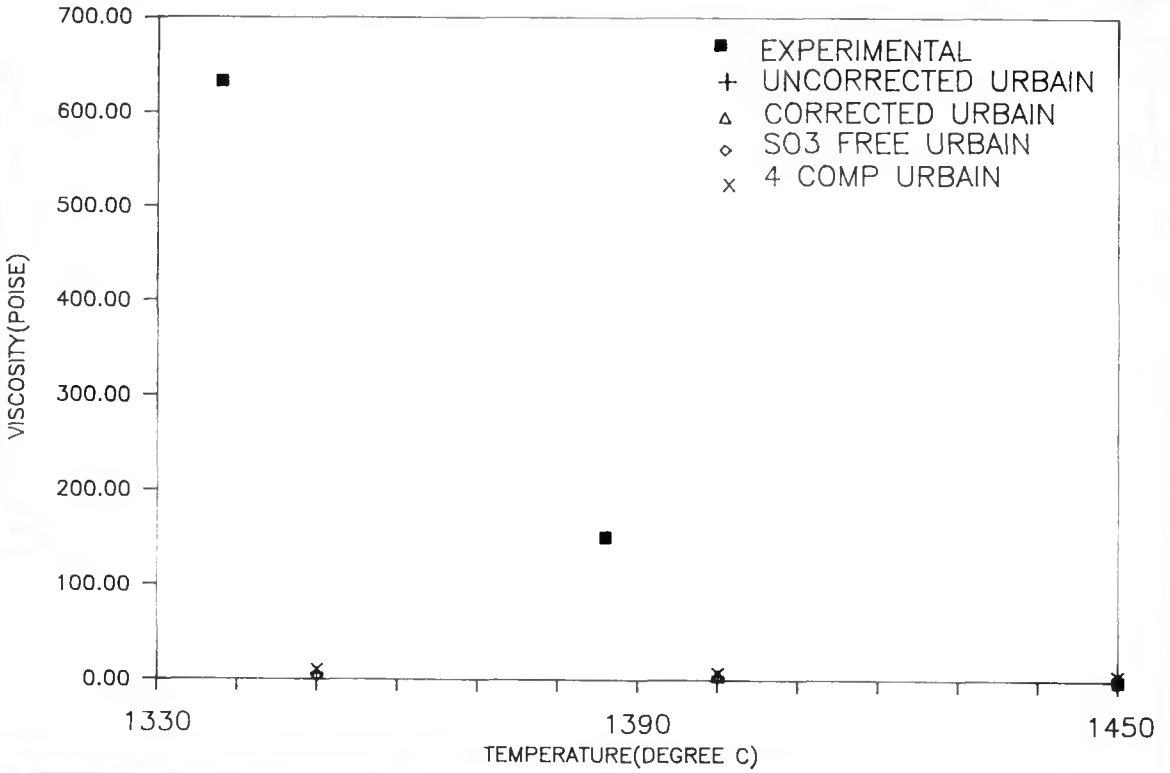

Figure 17. Comparison of Measured Viscosity With Various Models of Viscosity for Velva Coal (reducing atmosphere from reduced ash)

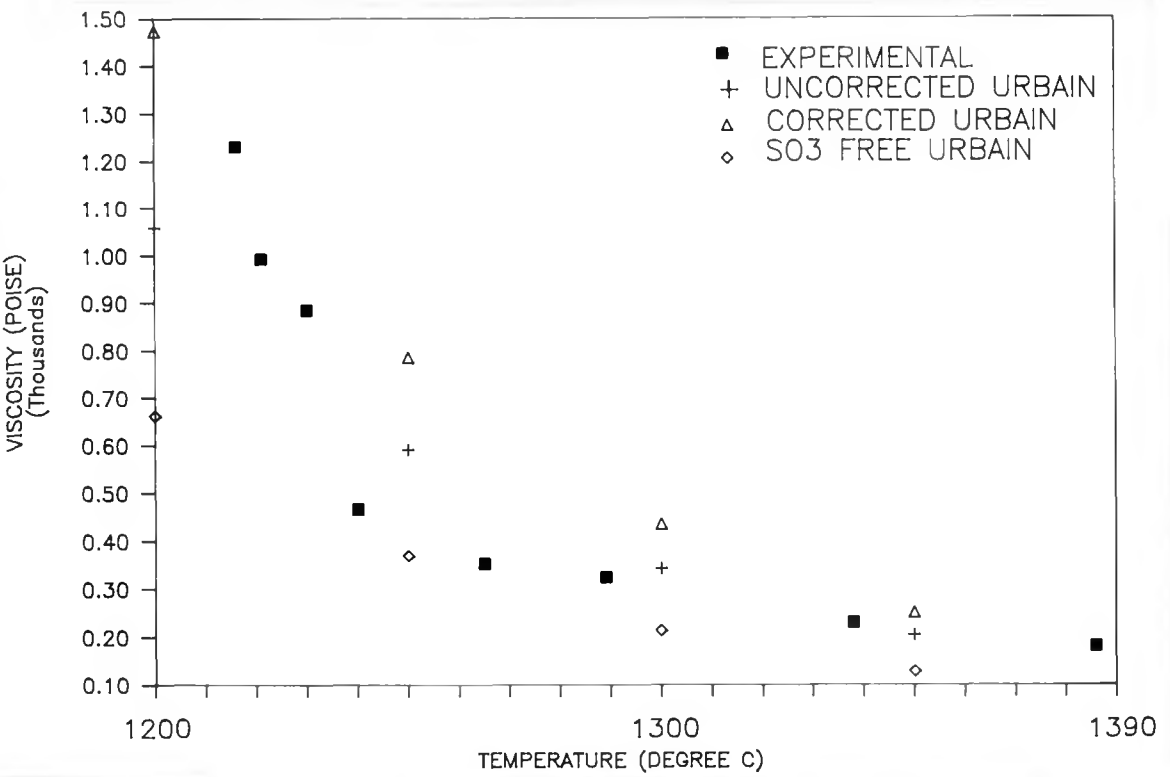

Figure 18. Comparison of Measured Viscosity With Various Models of Viscosity for Wyodak Coal (reducing atmosphere from reduced ash)

TABLE 8

SURFACE TENSION DATA

Sample	Surface Tension Data Treatment ASH:ATM	Temperature Degree C	Surface Tension Dynes/cm
Illinois No.6	OX:RED	1200	531
	RED:RED	1175	334
Indian Head	OX:RED	1225	530
	RED:RED	1195	481
Martin Lake	OX:RED	1315	590
	RED:RED	1275	337
Pittsburgh No.8	OX:RED	1275	483
	RED:RED	1275	358
Velva	OX:RED	1455	550
	RED:RED	1415	632
Wyodak	OX:RED	1265	844
	RED:RED	1260	713
Na-Montmorillonite	RED:RED	1345	293

5.0 FUTURE WORK

Detailed modeling efforts will be a major aspect of the third year of this project. Outstanding pressure pyrolysis, model mineral mixtures transformation, viscosity, and surface tension studies should be completed in the next quarter. This data is necessary to establish rigorous correlations of the experimental results.

6.0 REFERENCES

1. Raask, Erich, 1985. "Mineral Impurities" in Coal Combustion, Hemisphere Publishing Corp., Washington, pp. 484.

2. Schobert, H.H., R.C. Streeter, and E.K. Diehl, Fuel, 1985, 64, 1611.

3. Watt, J.D. and F. Fereday, Fuel, 1969, 42, 99.

4. Reid, W.T. and P. Cohen, Trans. American Society of Mechanical Engineers, 1944, 66, 83.

5. Frenkel, J.J., "Viscous Flow of Crystallizing Bodies Under the Action of Surface Tension," Jour. Phys. (Moscow), 9, 385.

6. Hastie, J.W., and D.W. Bonnel, "A Predictive Phase Equilibria Model for Multicomponent Oxide Mixtures Part II: Oxides of Na-K-Ca-Mg-Al-Si," High Temperature Science, 1984, 19, (3), 275.

7. Stewart, G. et al., Computer Modeling and Analysis of Chemical Processes from Coal Conversion Streams and Related Experiments - Final Technical Report, Sept. 1981, Contract No. DE-AC21-79-MC11783.

8. Sage, W.L. and J.B. McIlroy, "Relationship of Coal Ash viscosity to Chemical Composition," Journal of Engineering Power, 82, 1960, 145-155.

9. Kalmanovitch, D.P., S. Ness, and J. Weinmann, "Gasification Ash and Slag Quarterly Technical Progress Report for the Period of Oct. - Dec. 1987," DE-FC21-86MC10637.

10. Urbain, G., F. Cambier, M. Deletter, and M.R. Anseau, Trans. J. Br. Ceram. Soc., 1981, 80, 139.

11. Kalmanovitch, D.P., and J. Williamson, "Crystallization of Coal Ash Melts," Mineral Matter and Ash in Coal, ACS Symposium Series 301, ACS, Washington, D.C., 1986, p. 234-255.

12. Ness, R.O., Research Engineer, University of North Dakota Energy and Mineral Research Center, Jan. 1988, Personal Conversation (701-777-5000).

13. Kozakevitch, P., "Tension Superficielle et Viscosite des Scoues Synthetics," Rev. de Melatturgis, 1949, 46, pp. 505-516 and 572-582.

APPENDIX

CHARACTERIZATION OF ASHES, AGGLOMERATES, AND CLINKERS FROM COAL GASIFICATION UNITS

The important aspect of this program is the relationship of the laboratory-scale results to the formation and behavior of ash and slag in coal gasification units. The coals chosen in this project are the same as those which are part of the test matrix of the hydrogen production fluidized bed gasifier at EMRC. Agglomerates formed during various tests while operating the gasifier were analyzed by the techniques used to characterize the ashes and slags produced in this project. The focus of the characterization was the determination of the species which were responsible for the agglomeration.

The test matrix used in the hydrogen production project involves the use of six coals and a series of bed materials and catalytic additives. The bed materials used have included quartz, limestone, and gabbro (a fine-grained granite). Significant agglomeration was observed at low temperatures (700° to 800°C) in the quartz bed with added trona. The analysis showed that melting between the silica and the trona formed liquid phases of low viscosity at the average bed temperature. Furthermore, the product, a high sodium silicate liquid, would, on the basis of the surface tension results of this study, have a very low surface tension. The combined effect of low viscosity and low surface tension of the liquid phase present on the surface of the particles would facilitate extensive sintering and formation of agglomerates. The conclusion of the study was that quartz was not suitable as a bed material when trona was used as a catalyst due to the extensive melting and subsequent sintering of particles. Studies of a limestone bed with added trona also showed agglomeration. Examination and characterization of the agglomerates using x-ray diffraction and scanning electron microscopy revealed an interesting result: the sodium carbonate (trona) formed an intimate mixture with the calcium oxide and carbonate. This was revealed by SEM analysis which showed interfacial regions containing both sodium and calcium. X-ray diffraction analysis, however, showed calcium and sodium carbonate were present with no evidence of a product of reaction between the sodium and carbonate. Further analysis of other samples and other experiments have indicated that the trona may only be used in a gasifier at temperatures below 700°C. Above this temperature, the trona melts and reacts readily with bed material and ash. Tests involving gabbro with the trona have shown that the sodium carbonate can cause agglomerates with the relatively inert gabbro. Research is ongoing to determine the agglomeration mechanism of the gabbro.

A further set of ashes and agglomerates was obtained from the Lurgi gasifiers at the Great Plains Gasification Project. The gasifiers were experiencing a number of operating problems. The first was excessive clinkering of ash in the gasifier. The second problem was the poor gasifier output for some coals. As part of a separate DOE project, studies were undertaken to understand the clinkering problem and the effect of coal characteristics to coal gasification. Analysis of clinkers showed that sodium and calcium-rich liquid phases had formed in the ashes which were responsible for the formation of the clinkers. The liquid phases were of low melting point and of low viscosity. Based on the analysis, it was concluded that the clinkering problem was due to the use of coals with a high sodium content. Because of this, the operators restricted coals with an excessively high sodium content. Other research has been undertaken to understand the potential role of additives in reducing excessive clinkering. This work is still in progress.